



UNIVERSITY
OF MANITOBA

MECH 4860 - Engineering Design
Final Design Report
Team 17: Ossa Surgical
Kerrison Rongeur Redesign



Ossa Surgical

Timothy McAllister

Cory Neill

Kristopher Geyson

Robert Boresky

Project Advisor: Dr. T. ElMekkawy



Winnipeg Regional Health Authority
Office régional de la santé de Winnipeg
Caring for Health À l'écoute de notre santé



Health Sciences Centre
Winnipeg

Abstract

This report outlines the redesign of a Kerrison surgical instrument used by surgical staff at the Winnipeg Health Sciences Center (HSC). The primary goal of the redesign was to strengthen the current instruments while maintaining the vitally important ease of sterilization. Our team was also requested to determine any notable causes of failure in the current instruments.

It was determined through physical testing and computer analysis that a significant weakness was evident in the cutting tip of the Kerrison. The center of the crossbar was noted to experience relatively high tensile strain along the top portion causing a bowing effect that was noticeable by the technical staff at HSC.

Our redesign of the Kerrison comprises several new elements. These include multiple stages of sharpening to improve the service life of the instrument, a set of handles with varying geometries to accommodate the stage sharpening, and a redesigned hand rest for improved comfort. The material of the Kerrison was also altered to 420 martensitic stainless steel containing Molybdenum along with Titanium Nitride and Zirconium Nitride coatings to improve durability and corrosion resistance.

Finite element analysis (FEA) was performed on a computer model of our redesigned Kerrison showing that the stresses experienced in various locations were reduced due to the stronger material that was chosen. During the FEA it was determined that a reduction in the height of the blade did not contribute significantly enough to a reduction in stress to warrant altering the geometry.

Our design has been determined to fulfill the objectives set by our client. Consideration of the various elements in our design would lengthen the service life of the Kerrison while still being able to be easily accommodated in the current sterilization techniques at HSC [1-2].

Table of Contents

List of Figures	iii
List of Tables	vii
Glossary of Terms	viii
1 Introduction	1
1.1 Customer Requirements	1
1.2 Problem Statement	2
1.3 Project Objectives	2
1.4 Project Scope	2
2 Description of Current Models	3
3 Testing and Analysis of Current Designs	5
3.1 Known Issues with Current Kerrison Models	5
3.2 Strain Gage Testing and Finite Element Analysis	7
3.2.1 Experimental Setup	7
3.2.2 Experimental Results	11
3.3 3D Modelling	19
3.4 Old Kerrison Model	20
3.5 Current Kerrison Model	21
3.6 Material Testing	22
3.7 Factors not considered	35
3.7.1 Foot Plate Deformation:	35
3.7.2 Torque and twisting:	36
3.7.3 Biting of tissue:	36
4 Redesign of Kerrison Rongeur	36

4.1	Overview	36
4.2	Handle Redesign	37
4.2.1	Linear Transfer Mechanism.....	37
4.2.2	Staged Sharpening with Multiple Handles	39
4.3	Hand Rest Redesign	40
4.4	Blade Height Reduction	42
4.5	Material and Coating Selection	46
5	Analysis of Redesigned Kerrison	48
5.1	3D Modeling	48
5.1.1	Assembly.....	49
5.2	Finite Element Analysis of Crossbar.....	50
5.3	Force Transfer Analysis	53
5.4	Finite Element Analysis of Handles.....	57
5.5	Sterilization Compatibility	60
5.6	Cost Analysis.....	61
6	Conclusion.....	63
7	References	64
	Appendix A – Concept Selection.....	65
	Appendix B – Strain Gage Specifications	68
	Appendix C – Search Results	69
	Patents.....	69
	Competitor Products	69

List of Figures

Figure 1. Overview of Kerrison components.....	3
Figure 2. Strain gage locations on Kerrison test instrument.....	6
Figure 3. Tip Deformation due to excessive loading while biting a hard material, used with permission.....	6
Figure 4. Bowing of the crossbar due to excessive loading, used with permission.....	7
Figure 5. Experimental apparatus of strain gage and load cell testing.	8
Figure 6. The location of the two strain gages that measure strain in the crossbar as force is applied to the handle.	8
Figure 7. The 500 lb load cell used in the experiment to measure the bite force during testing. ...	9
Figure 8. Depiction of how the 0.5" nut was used to transfer force from the cutting tip to the load cell.....	10
Figure 9. Placement of a 0.5" nut between the Kerrison's tip and the load cell.....	10
Figure 10. Picture or force being applied to the Kerrison's handle during Trial 3 of the experiment.....	11
Figure 11. Experimental data for all five tests showing Force in green, tip strain in blue and middle crossbar strain in red.	12
Figure 12. Graph of Force vs. Strain for Trial 1.	12
Figure 13. Kerrison crossbar tip just as it is about to be loaded.	13

Figure 14. Kerrison after it has been fully loaded causing a compressive force on the strain gage.	14
Figure 15. FEA simulation of the centre of the crossbar displacement under tip loading.....	15
Figure 16. Graph of Force vs. Strain for Trial 2.	16
Figure 17. Graph of Force vs. Strain for Trial 3.	17
Figure 18. Graph of Force vs. Strain for trial 4.	18
Figure 19. Graph of Force vs. Strain for Trial 5.	19
Figure 20. Non-detachable Kerrison crossbar.	20
Figure 21. Non-detachable Kerrison shank.	20
Figure 22. Non-detachable Kerrison handle.	21
Figure 23. Adjustable Kerrison crossbar.	21
Figure 24. Adjustable shank.	22
Figure 25. Adjustable handle.	22
Figure 26. V. Mueller Kerrison with material sample cuts.....	24
Figure 27. V. Mueller Kerrison with samples removed.....	24
Figure 28. V. Mueller Kerrison cross sectional sample.....	25
Figure 29. V. Mueller Kerrison surface sample.....	25
Figure 30. Scanning electron microscope photograph of Kerrison cross section.....	28

Figure 31. Session 1 Kerrison cross section Trial 3 material analysis spectrum.....	29
Figure 32. Scanning electron microscope photograph of Kerrison coating.....	29
Figure 33. Session 1 Kerrison coating Trial 1 material analysis spectrum.....	30
Figure 34. SEM photograph of material with composition analysis going from cross section to coating.....	32
Figure 35. Element presence going from cross section to coating.	33
Figure 36. Overview of redesigned Kerrison.....	37
Figure 37. Force transfer mechanism of non-detachable model.....	38
Figure 38. Force transfer mechanism of detachable model.	38
Figure 39. Designs for three stages of staged sharpening concept.	39
Figure 40. Hand rest of current Kerrison models.	41
Figure 41. Redesigned hand rest.....	42
Figure 42. Kerrison bite height comparison, used with permission	43
Figure 43. FEA of cutting tip with 3.5 mm bite height.....	44
Figure 44. FEA of cutting tip with 3.0 mm bite height.....	44
Figure 45. FEA of cutting tip with 2.5 mm bite height.....	45
Figure 46. FEA of cutting tip with 2.0 mm bite height.....	45
Figure 47. New crossbar height.	48

Figure 48. Curved Hand Rest.....	49
Figure 49. From left to right, stages 1, 2, and 3 of the redesigned Kerrison handles.	49
Figure 50. Assembly of crossbar, Shank and Handle.	50
Figure 51. Using FEA to identify stress concentrations in our design.	51
Figure 52: FEA of stresses in cutting tip with filleted key	51
Figure 53. Using FEA to examine the deformation of the mid section of the crossbar of the old Kerrison design.	53
Figure 54. Using FEA to examine the displacement of the mid section of the crossbar of the current Kerrison design.....	53
Figure 55. User-applied force components.....	54
Figure 56. Force transfer angle in rest position.	55
Figure 57. Force transfer angle in mid-cut position.....	56
Figure 58. Force transfer angle in fully-compressed position.	56
Figure 59. Stress distribution throughout the thin member of the first stage handle.....	58
Figure 60. Stress distribution throughout the thin member of the second stage handle.	59
Figure 61. Stress distribution throughout the thin member of the third stage handle.....	60
Figure 62. Detachable Kerrison showing opening ability for standardized cleaning and sterilization.....	61

List of Tables

TABLE I SESSION 1 CROSS SECTION ANALYSIS	26
TABLE II SESSION 1 SURFACE ANALYSIS	27
TABLE III SESSION 2 CROSS SECTION ANALYSIS	30
TABLE IV SESSION 2 SURFACE ANALYSIS	31
TABLE V COLOR KEY FOR ELEMENT PRESENCE GOING FROM CROSS SECTION TO COATING.....	34
TABLE VI TIP HEIGHT REDUCTION COMPARISON	46
TABLE VII 410 AND 420 MARTENSITIC STAINLESS STEEL PROPERTIES	47
TABLE VIII CUTTING TIP CONCEPT SCORING	65
TABLE IX CUTTING TIP CONCEPT KEY	66
TABLE X ERGONOMICS CONCEPT SCORING.....	67
TABLE XI ERGONOMICS CONCEPT KEY	67

Glossary of Terms

Kerrison: A tool used for bone and tissue cutting and removal in orthopedic back surgeries. The redesign of this tool is the focus of this report.

SEM: Scanning Electron Microscope, a tool used to observe material at a microscopic scale, and lower.

EDS: Energy Displacement Spectroscopy, a method of electron energy measurement to determine chemical composition of an object.

FEA: Finite Element Analysis, a numerical method of applying and analyzing stresses of a material

CSA: Canadian Standards Association, a governing body that sets and regulates various standards.

CAD: Computer Aided Design, a method of drawing and drafting in a two or three dimensional digital environment.

WRHA: Winnipeg Regional Health Authority, the client for this design report.

HSC: Health Sciences Centre, the site where the Kerrison studied in this report is used.

Strain Gage: An instrument physically applied to a geometry and used to measure localized strain due to applied stress.

Old Kerrison: The non-detachable Kerrison that was robust and durable but hard to clean and no longer in service at the Health Sciences Centre.

Current Kerrison: The detachable Kerrison that is easily cleaned and sterilized but suffers from cutting tip deformation.

New Kerrison: The proposed redesign in the following report of the current Kerrison.

1 Introduction

The Health Sciences Center (HSC) in Winnipeg, MB requires a surgical bone remover, known as a Kerrison, which is effective, easily cleanable, biodegradable, and durable in order to perform spinal surgeries. Our client is a clinical engineer who works with the HSC who has been focusing on the cleanliness and durability of the instruments as well as the procedures that take place at HSC. Our project fits into both of these categories. We will be redesigning the Kerrisons that are currently in use, and in the processes, not only increase its cleanliness and durability; but also address all concerns raised by our client of the previous models.

1.1 Customer Requirements

The needs that were mentioned in the previous section can be broken down into the two main categories: ease of cleaning and durability. The two models currently in circulation at HSC both fail due to one of the above mentioned criteria. The first Kerrison, made by Mueller, are robust, durable, and comfortable pieces of equipment that are currently the standard. The problem lies in the difficulty of cleaning the Kerrison. A technician is required for disassembly, which means it cannot be part of the standardized sterilization cycle. In order for the Kerrison to be cleaned thoroughly, it must be washed, sent to the technician for disassembly, washed again, sent back to the technician for reassembly, and washed a final time before entering sterilization. The steps added by forcing the Kerrison to be disassembled after each use not only makes the cleaning cycle longer, but also occupies the technician and prevents him from performing other required jobs. New Kerrisons were ordered with the goal of fixing this problem, however, HSC ran into several other unexpected issues with the tool. The new Kerrisons have a feature that allows them to be easily cleaned due to a latch that makes it possible to open the top of the Kerrison without requiring a technician. However, the new models have much lower durability and deform after only a couple of operations.

1.2 Problem Statement

Our Problem statement is as follows: to create a design for the Kerrison that is durable enough to withstand approximately 750 operations, knowing several hundred bites are performed per operation, without deformation. It must be easy to clean in order to fit into the standardized sterilization cycle. The force must be transferred adequately from handle to cutting edge without wasting energy. The Kerrison should be constructed of stainless steel containing molybdenum due to its cost effectiveness as well as its anti-corrosive properties while being comfortable and ergonomic.

1.3 Project Objectives

Our project objective is to solve several problems that HSC is facing with the current Kerrisons. The problem associated with the method of force transfer will be solved using our design by making it linear as opposed to radial. This will ensure the crossbar and shank of the Kerrison remain in contact throughout the entirety of the cut. To fix the deformation problem, our goal is to have the cutting tip's integrity maintained throughout countless operations by adjusting bite height and material choice. The tool must also be easily and thoroughly cleanable without requiring a technician. Finally, the ergonomics of the tool will be increased via a redesigned handle.

A CAD model is presented showcasing our new design accompanied by finite element analysis and material chemical composition testing in order to justify the changes and show that all the problems have been addressed. The design will comply with all CSA standards and the medical device regulations that are applicable to Class 1 surgical instruments. A comparison of the effects of the height of bite and the length of keyway of the older style Kerrisons have been performed to see if alterations in these areas have effects on performance, durability and deformation.

1.4 Project Scope

The specifications and measurements of our design will be based on the Kerrisons of 3mm blade width. The Kerrisons are available in sets that include 1mm, 2mm, 3mm, 4mm and 5mm sizes. The 3mm model was chosen as the test width since it's the most commonly used size during

orthoscopic surgeries. Our design must be durable in order to withstand repeated cuts through large cortical bones and tissue in the lower spinal area.

2 Description of Current Models

Figure 1 below depicts the key features of the current Kerrison models:

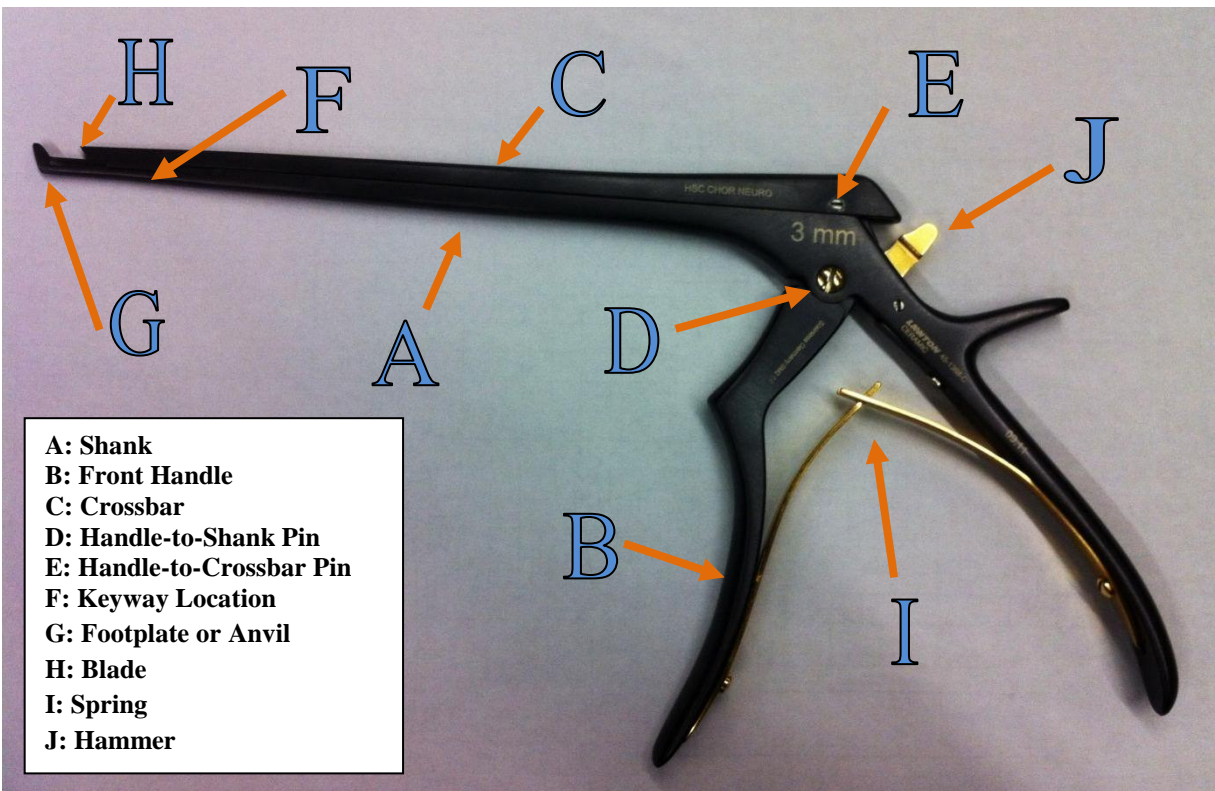


Figure 1. Overview of Kerrison components.

The main structures that comprise the Kerrison are the shank (A), front handle (B) and the crossbar (C). The handle is hinged to the shank by a pin connection at location D and the crossbar is hinged to the handle by a similar pin connection at location E. The crossbar is also affixed to the shank by keys located near the cutting tip and near the handle pin.

The keyway at location F has a major role in the assembly of the Kerrison. The keyway essentially acts as a guide for the crossbar; it constricts the motion of the crossbar relative to the shank. This is done through the use of two interlocking parts. Once the keyways are inserted into

their respective slots and force is applied onto the handle, the keyway stops the crossbar from rising off the shank. The keyway will also restrict the crossbars lateral movements relative the shank keeping the assembly inline. The size of the keyway and the material used for construction will affect the durability of keyway and the magnitude of load it is capable of regulating.

The cutting tip comprises both an angled footplate or anvil at the end of the shank (G) and an angled blade on the moving crossbar (H). Both of these components are angled forward so that the surgeon is able to angle the entire tool downwards in order to gain a better view of the material being cut. A vertical cutting edge would be less practical since the entire tool would have to be held vertically, or the cutting mechanism would have to be placed under the material, potentially damaging surrounding material.

The crossbar cutting tip also houses a small chamber approximately 2mm in length behind the blade. The purpose of this chamber is to allow temporary storage of material buildup and subsequently decrease stress on the blade. The built-up material is immediately released or washed out after retracting the blade.

The spring (I) is used to retract the handles after the user has finished compressing the front handle. This is needed since the tool does not have looped handles as scissors do in order to open and close the cutting blades. This two piece spring back design is commonly used on other Kerrison models and is considered to be the industry standard design.

There is a hammer located on the back on the Kerrison at location J, which when pulled, allows for the crossbar to detach from the shank. This is an important feature as the ability to separate the crossbar from the shank allows the Kerrison to be incorporated into the standard sterilization cycle (discussed in further detail in section 5.5.5). The hammer, when closed, has a latch that prevents the crossbar from sliding far enough back for the keyways to leave their guides; this forces the contact between the crossbar and shank. When the hammer is pulled, the keyways can slide far enough to get past the guides and thus allowing for the opening of the Kerrison.

3 Testing and Analysis of Current Designs

The testing and analysis of the current Kerrison instrument was comprised of two components: strain gage testing and finite element analysis (FEA). Finite Element Analysis is an extremely valuable modeling tool for projects that involve stress, strain, or displacement of objects being subjected to loads of any kind. FEA allows the user to apply a wide variety of forces such as torque, tension, and compression to a CAD-created 3D model. FEA software also allows you to specify your material properties, which is vital to obtaining accurate results. This simulates real world loading and allows the user to understand how an object will be affected by the applied loads.

In the case of a Kerrison surgical tool, FEA allows us to analyze how the tool will react when experiencing heavy loading that is involved in cutting bone and tissue during lower back surgery. FEA points out the areas that are likely to fail such as stress concentrations, as well as identifies where material needs to be added for strength, and where excess material can be removed. FEA was not used extensively in the testing of the existing models, but rather to confirm the experimental results from the strain gage testing. FEA is utilized in a greater capacity when analyzing our final design concepts since we will not have a prototype to perform physical tests on.

3.1 Known Issues with Current Kerrison Models

Kerrisons experience heavy loading that often leads to deformation over time. It has been indicated by the clients that two key areas have exhibited deformation on a regular basis. The two main areas of concern are the cutting tip (A) and the mid crossbar region (B) of the Kerrison show in Figure 2 below. Section A has been found to deform sooner and more often than section B. Section A's deformation is much more detrimental to the use of the tool.

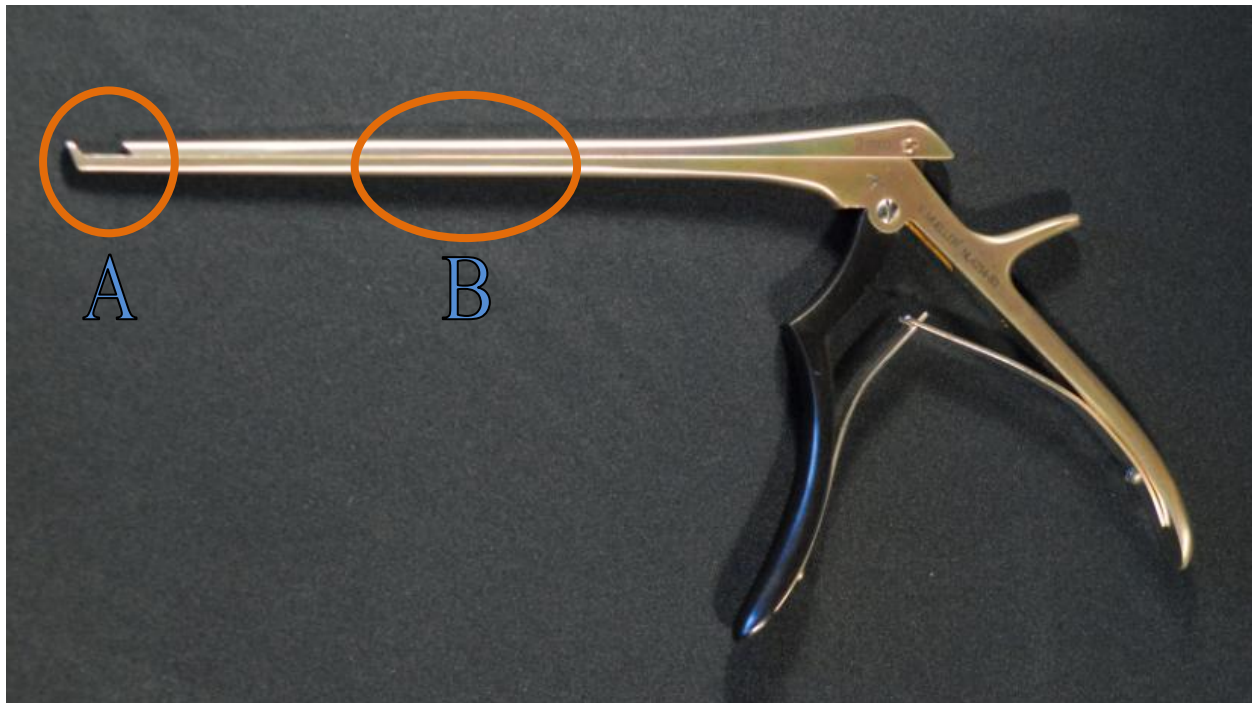


Figure 2. Strain gage locations on Kerrison test instrument.

This section of the report will contain experimental testing of the loads that the current Kerrison can withstand to explain why the current tools are failing the way that they are. Shown on the next page are two examples of how the existing Kerrison is failing. Figure 3 shows how the cutting tip is being bent upwards over time as the force of the material being cut pushes back on the cutting tip; while Figure 4 shows gap formation between the crossbar and the shank in the middle portion of the crossbar.

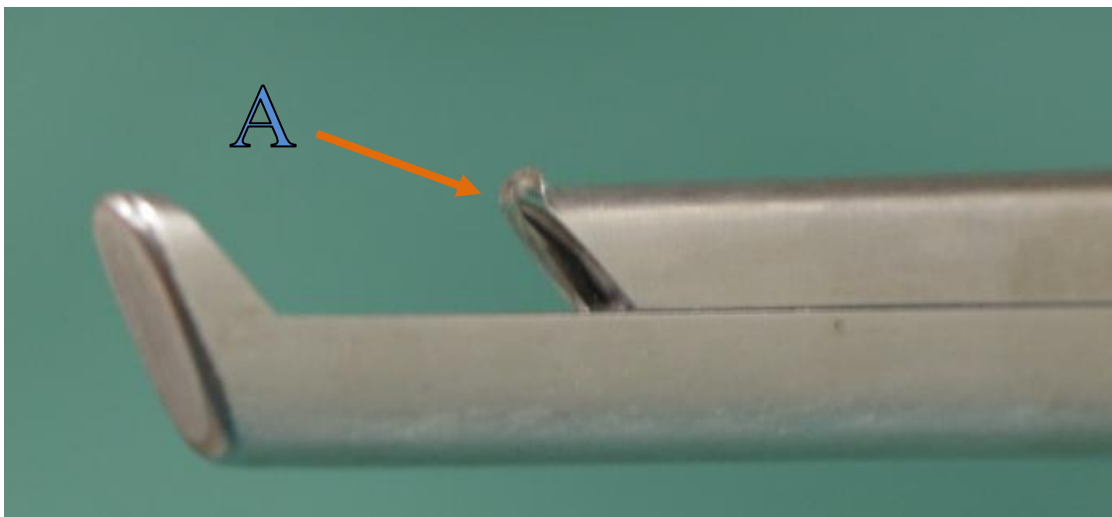


Figure 3. Tip Deformation due to excessive loading while biting a hard material, used with permission. [3]

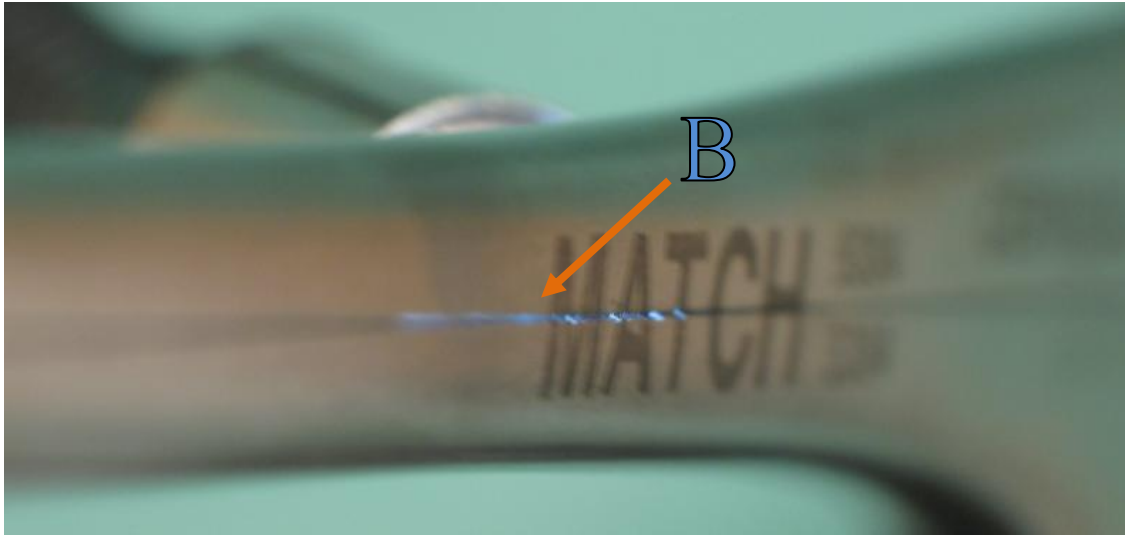


Figure 4. Bowing of the crossbar due to excessive loading, used with permission. [3]

3.2 Strain Gage Testing and Finite Element Analysis

The physical testing of the current Kerrison model comprised the use of multiple strain gages applied to separate areas of the instrument. Using strain gages and recording software, results were able to be obtained. FEA software was then utilized to verify the experimental results obtained from the testing.

3.2.1 Experimental Setup

The objective of experiment 1 is to calculate the strain throughout the crossbar when the tool is being loaded up to a 100 kg bite force. A 100 kg bite force is approximately the maximum the average male can produce with the grip of a single fist. This experiment involved the use of 2 strain gages with specifications listed in appendix B, a 500 lb load cell, 7 various clamps, 1 computer, and one 0.5” stainless steel nut. Figure 5 below show the complete setup of the experimental apparatus.

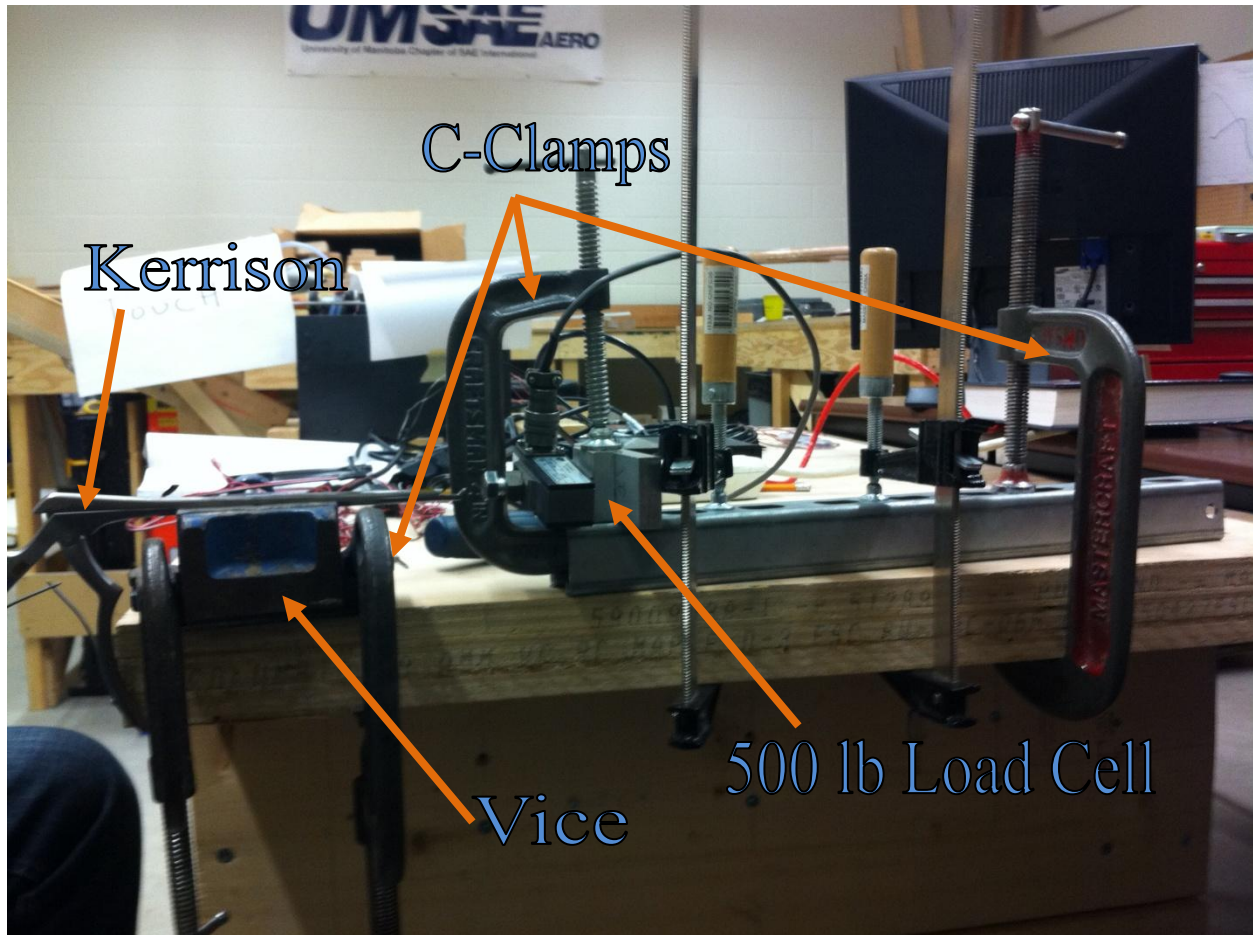


Figure 5. Experimental apparatus of strain gage and load cell testing.

Experiment 1 is comprised of an apparatus that holds the shank in place while allowing a force to be applied to the handle. This force is transferred from the handle, through the crossbar, and applied to the cutting tip of the Kerrison.

Figure 6 below shows where the strain gages were applied to the Kerrison. The strain gages were applied in these particular locations because they have shown signs of deformation in the past. Point B is at the tip of the crossbar, while Point A is in the middle of the crossbar.

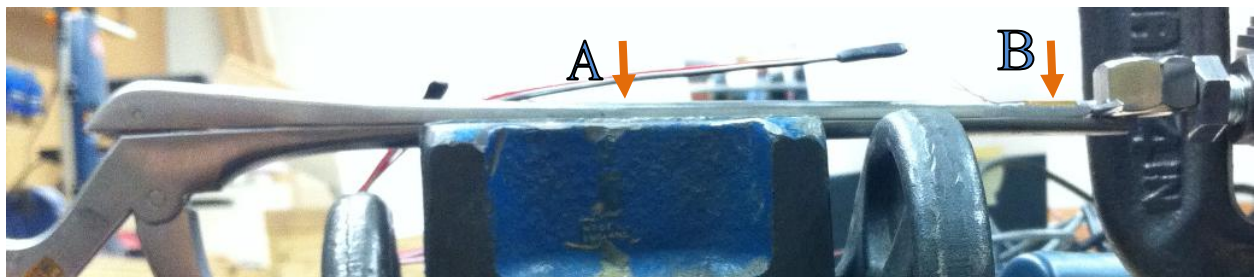


Figure 6. The location of the two strain gages that measure strain in the crossbar as force is applied to the handle.

Figure 7 below shows the experimental set up of the 500 lb load cell that is used in Experiment 1 to measure the bite force being applied. This is needed to correlate the strain experienced by the cross bar with the amount of force applied to the tip at any instance in time.



Figure 7. The 500 lb load cell used in the experiment to measure the bite force during testing.

A big challenge was to find a way to measure the biting force of the cutting tip (point A) of Figure 8 below. The anvil end (point B) of the shank got in the way of directly pushing against the load cell (point C). This was solved by using a 0.5” stainless steel nut, placed between point A and point C while allowing the anvil (point B) to sit in the open space at the centre of the nut.

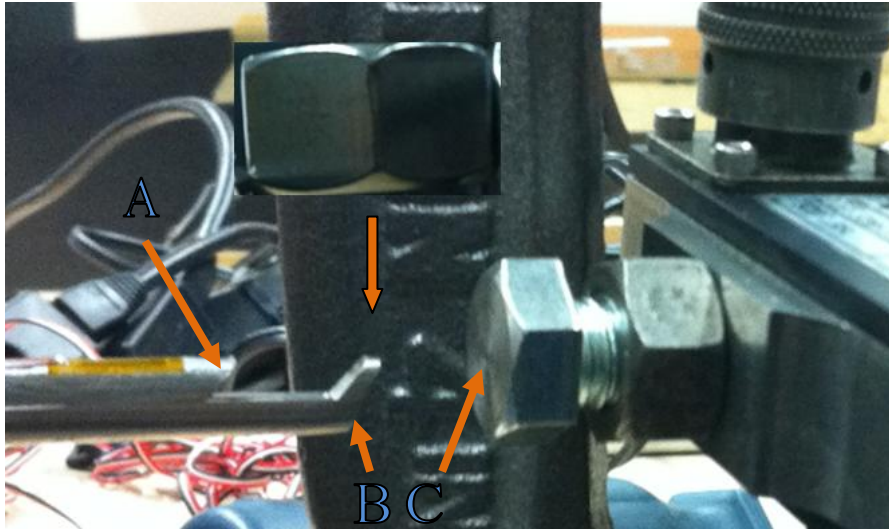


Figure 8. Depiction of how the 0.5" nut was used to transfer force from the cutting tip to the load cell.

Figure 9 is showing the nut in its desired position allowing full force transfer between points A and C. The nut must be made from a rigid material so that a true force value will be transferred fully from the tip into the load cell. If a nut made from a softer material was used, some of the force would have been lost inside the nut as it deformed.

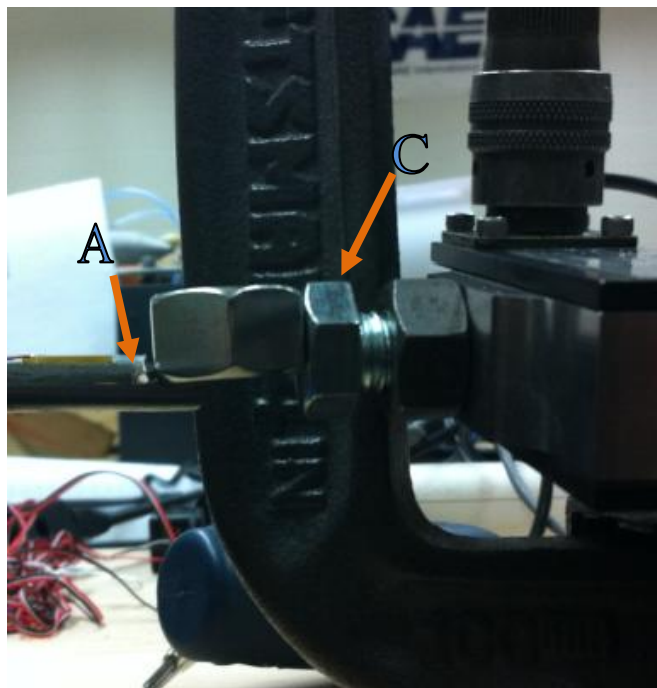


Figure 9. Placement of a 0.5" nut between the Kerrison's tip and the load cell.

An iOTech 6224 data acquisition system was used to collect the load cell data as well as the two strain gages data. Using Encore software, we were able to measure the bite force, and the strain experienced in each strain gage simultaneously.

3.2.2 Experimental Results

Five trials were conducted in order to gain the best results possible. A member of ‘Ossa Surgical’ Team 17 used his hand to apply a force onto the handle of the Kerrison. Each Trial consisted of starting from zero force applied, then up to the maximum force he could apply, and then slowly back down to zero force. Figure 10 was taken during trail 3 of this experiment. A force was applied to the handle at A, and the force was transferred through a pin joint at B down through the cross bar and into the Nut and load cell set up at point C.

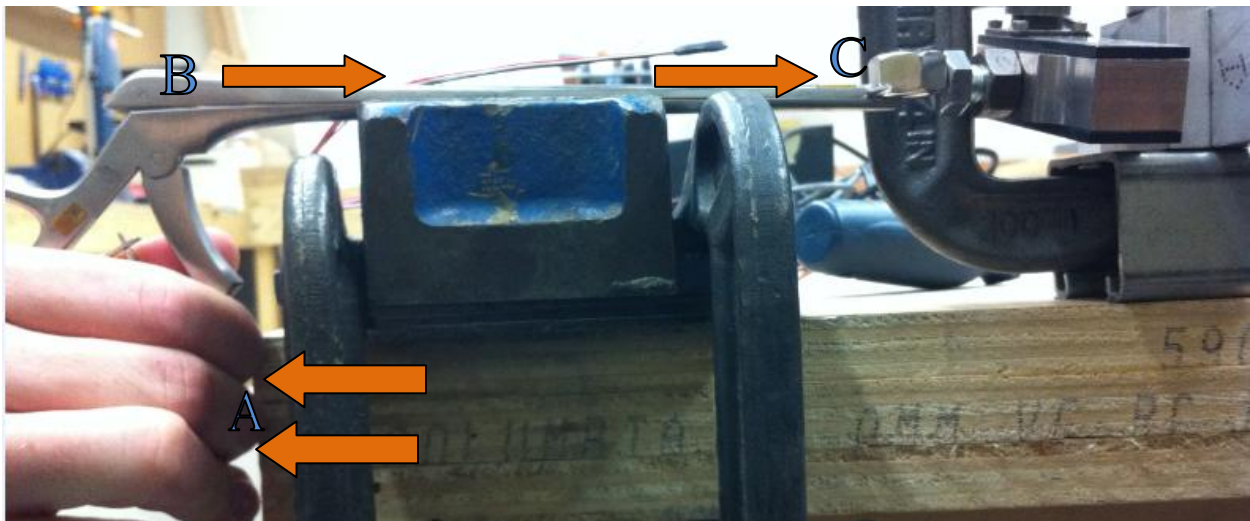


Figure 10. Picture of force being applied to the Kerrison's handle during Trial 3 of the experiment.

The five trials took place over a 5 minute time span and over that time the data acquisition system recorded strain and force values at 500,000 different instances. This data was then imported into excel and used to graphically demonstrate what the strain gages were experiencing during each Trial. Figure 11 represents the data for all five trials. The green line represents the application and removal of force. Each corresponding blue and red line represents the given state of strain that each of the strain gages are experiencing at that particular moment in time. This graph is used to give an idea as to what we are expecting the gages to do.

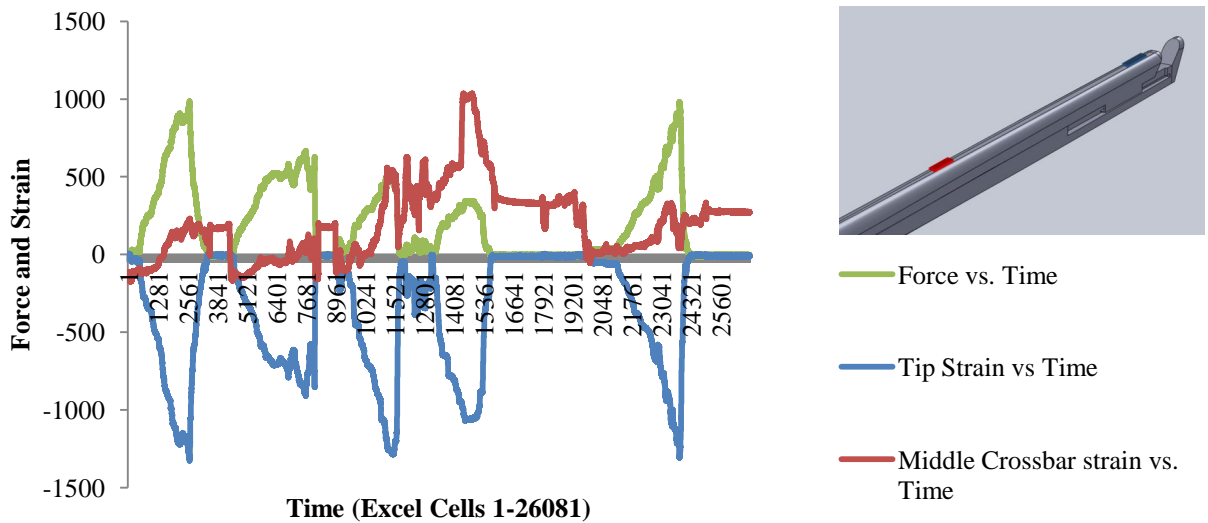


Figure 11. Experimental data for all five tests showing Force in green, tip strain in blue and middle crossbar strain in red.

Further graphical data is shown in the subsequent sections in terms of plots of Force vs. Strain for each individual Trial.

3.2.2.1 Trial 1

Figure 12 shows the relationship between force and strain at both gage locations on the crossbar for Trial 1.

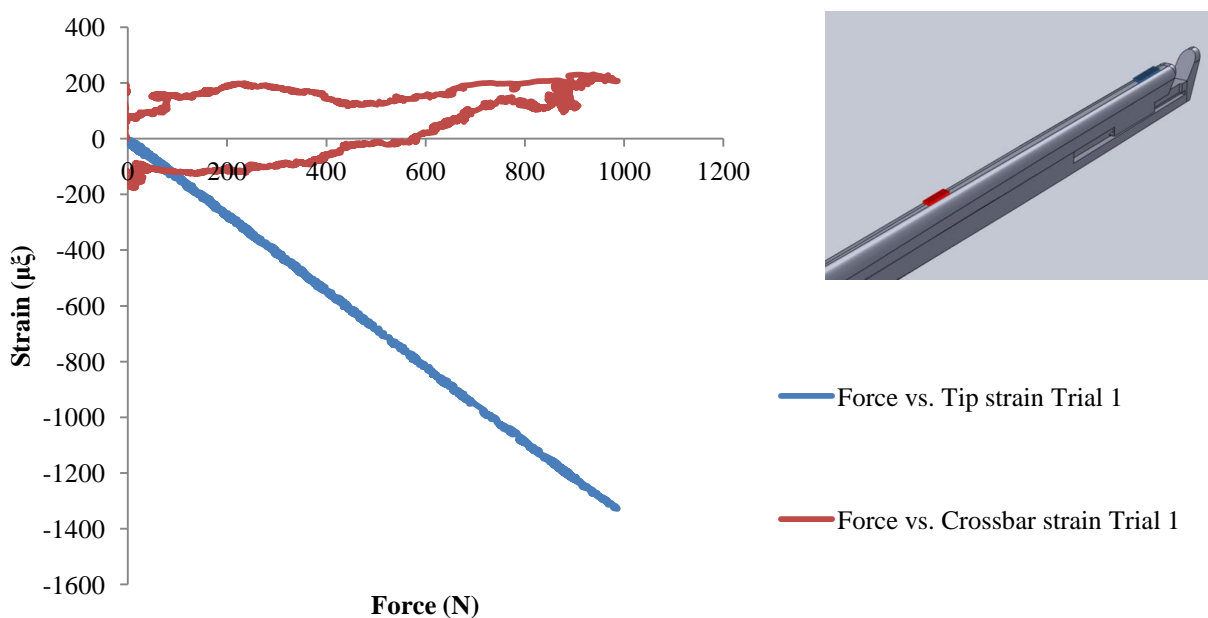


Figure 12. Graph of Force vs. Strain for Trial 1.

As originally expected, the tip strain gage experiences a linear relationship between force and strain. Notice that the blue line is linear up to 1000N and then follows the same path as the Kerrison is unloaded. Since the blue line is in the negative strain region the strain gage would have been experiencing only compressive strain. Compressive strain was expected because the angle of the cutting tip causes the force to be applied in the upward direction combined with the downward force the keyway. Figure 13 shows a model of the tip of the Kerrison's crossbar just as it is about to be loaded. The green arrows represent the force holding the keyway down by the shank. The purple arrows represent a load being applied to the tip when a material is being cut .

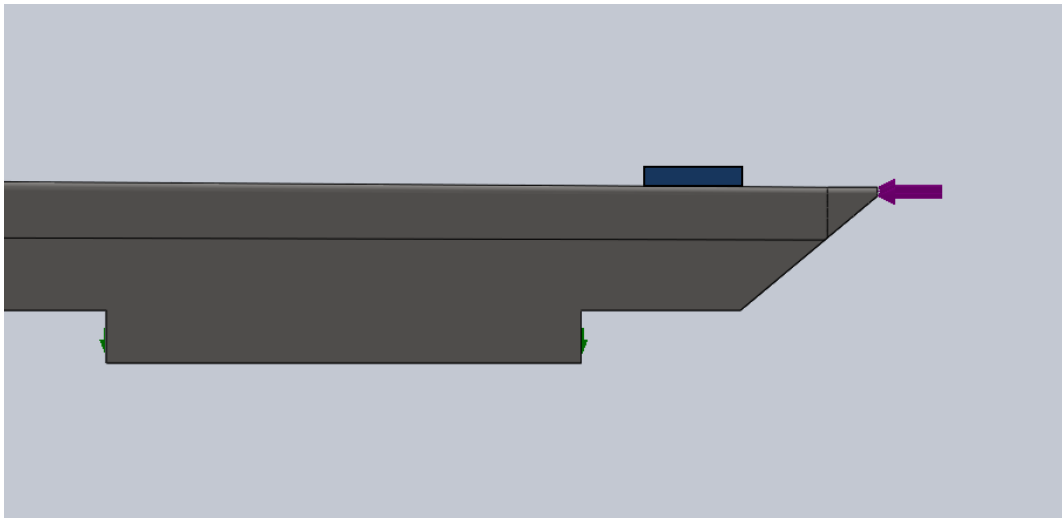


Figure 13. Kerrison crossbar tip just as it is about to be loaded.

We were able to confirm the experimental results using FEA shown in Figure 14. This simulation shows how the crossbar will strain under such loading, causing compressive or negative strain readings on the strain gage on top of the cutting tip.

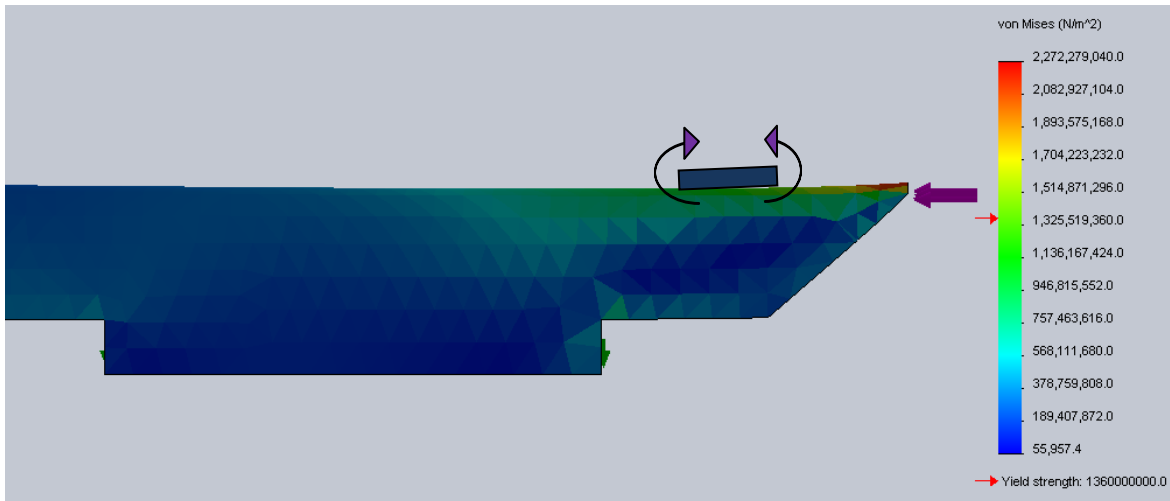


Figure 14. Kerrison after it has been fully loaded causing a compressive force on the strain gage.

The red line in Figure 12 shows that the strain data collected by the gage located in the middle of the crossbar is not nearly as linear, but does represent what was expected. The strain starts out as negative or compressive and once the load reaches a certain level the strain becomes positive or tensile strain.

This can be explained by looking at the design of the crossbar. There is one sliding keyway near the tip of the crossbar and a fixed hinge pin at the back connecting to the handle. The middle of the crossbar first experiences compression until the force gets too high. At high forces the crossbar wants to buckle in the centre. Since the loads are not large enough to cause complete buckling, the crossbar bows upward slightly in the middle of the keyway and the pin, which over time can lead to plastic deformation. Below in Figure 15, you can see an FEA simulation of how the centre of the crossbar wants to bow upward during heavy loading. Using the scale on the right side of the image, you can see the dark red in the centre of the crossbar represents the largest displacement in the positive upward direction.

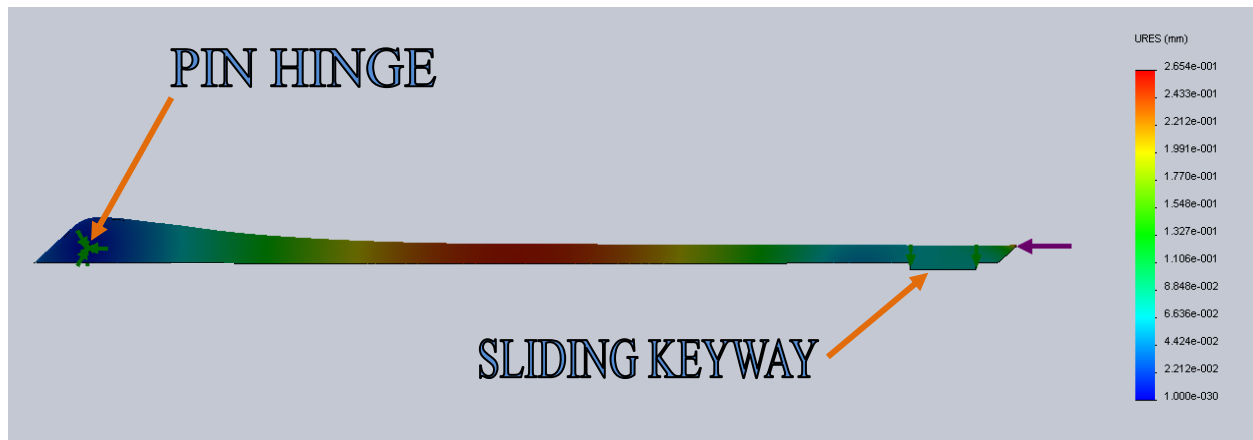


Figure 15. FEA simulation of the centre of the crossbar displacement under tip loading

Since the tip experiences nearly five times the amount of strain as the middle of the crossbar, it is likely that the tip will plastically deform much sooner than the middle of the crossbar. This explains why the clients have found many examples of tip deformation, and only a few examples of mid crossbar deformation.

3.2.2.2 Trial 2

Figure 16 shows a graphical representation of data collected during Trial 2. This data looks very similar to Trial 1. The strain shown at the tip is linear just as trial 1 was, but the force applied only reaches approximately 700N while Trial 1 reached 1000N. The strain shown in the middle of the crossbar follows a similar winding path as Trial 1, but due to the lower force applied, the tensile strain is not as high as Trial 1.

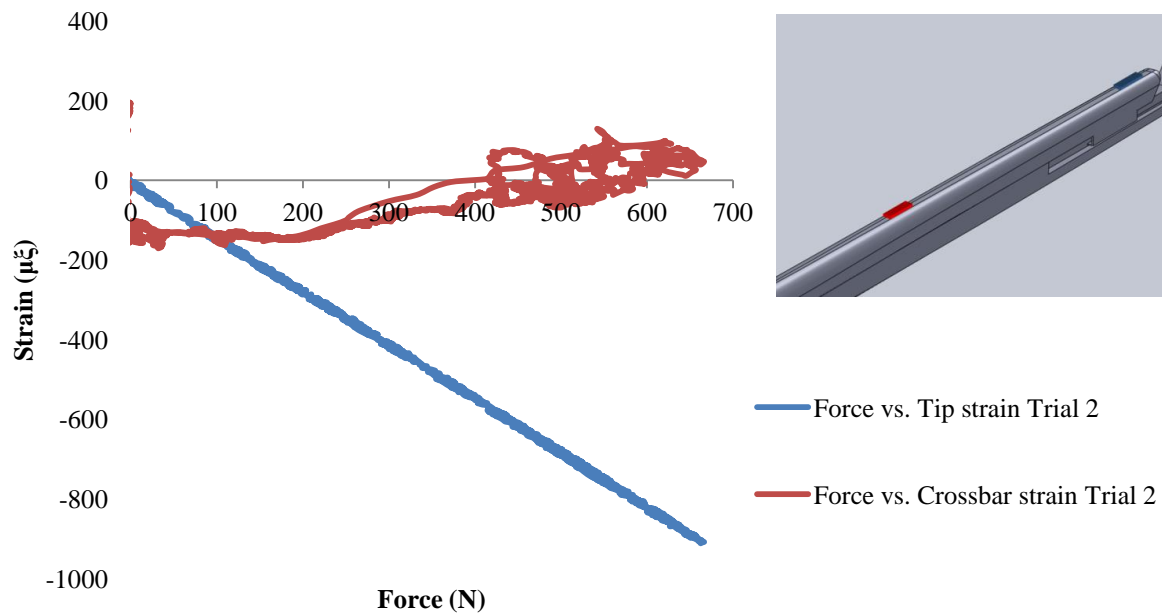


Figure 16. Graph of Force vs. Strain for Trial 2.

3.2.2.3 Trial 3

Trial 3 is where the first significant change occurred. Looking at the blue line in Figure 17 it can be seen that the loading and unloading are both linear, but they are offset from each other. During this trial it was noted that the very tip of the cutting edge began to curl back due to the heavy force applied directly to it. This plastic deformation of the tip caused an added amount of compressive strain onto the strain gage resulting in the change in path when unloading.

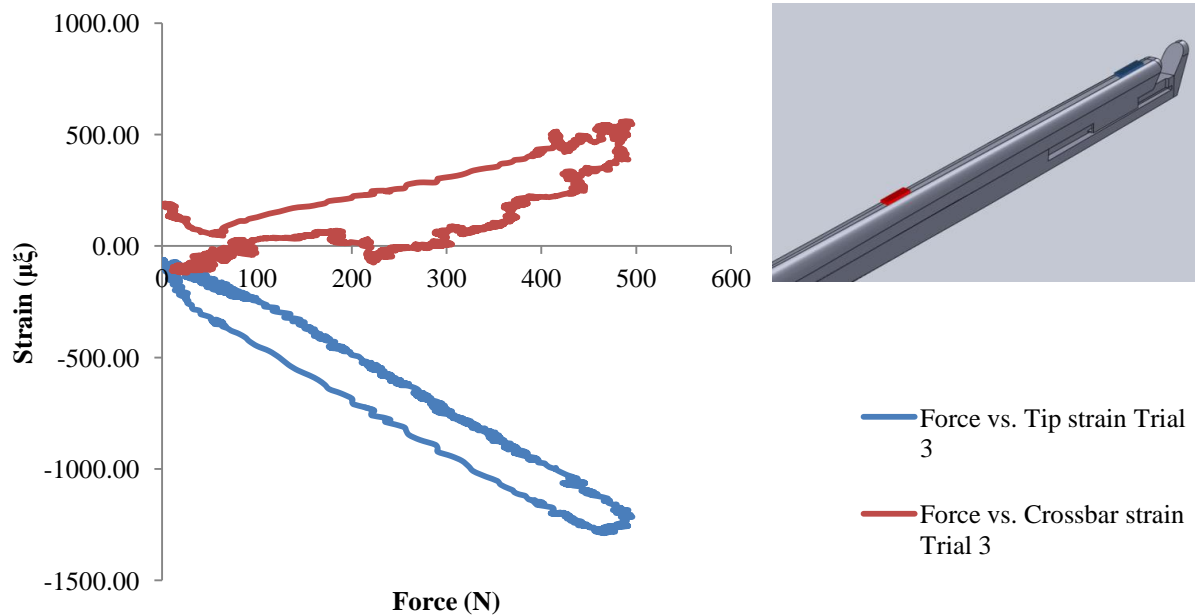


Figure 17. Graph of Force vs. Strain for Trial 3.

3.2.2.4 Trial 4

Data collected from trial 4 looks ambiguous and does not exactly agree with the previous three trials. Figure 18 shows a similar Force vs. Tip strain (blue line) as seen in trial 3 where there is an offset between loading and unloading. This is due to further deformation of the tip occurring during the loading. The biggest difference is seen in the mid crossbar strain. During each of the three previous trials, the mid crossbar strain starts as negative or compressive and as the load is increased, the strain becomes positive. In the case of trial 4 we see that the strain starts off at a positive value and never goes below $350 \mu\epsilon$.

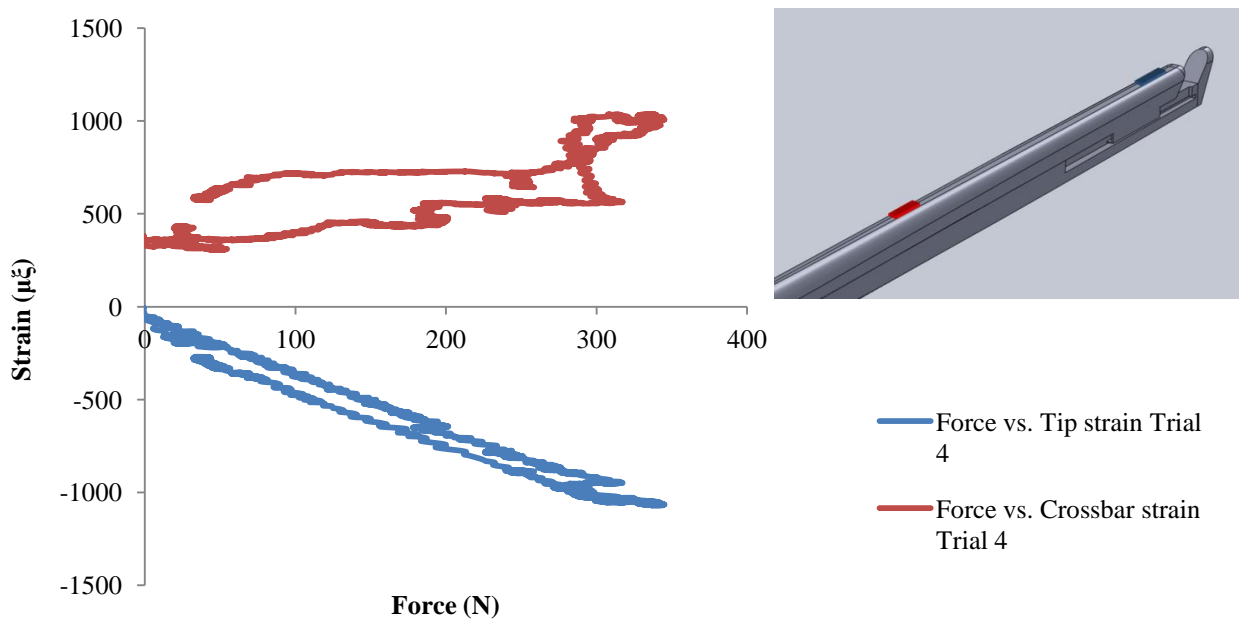


Figure 18. Graph of Force vs. Strain for trial 4.

3.2.2.5 Trial 5

Similar to trial 4, the red line shows that the crossbar strain starts in tension and is not in compression as was seen in trails 1 through 3. This leads us to believe that plastic deformation has occurred during trail 3 along the crossbar.

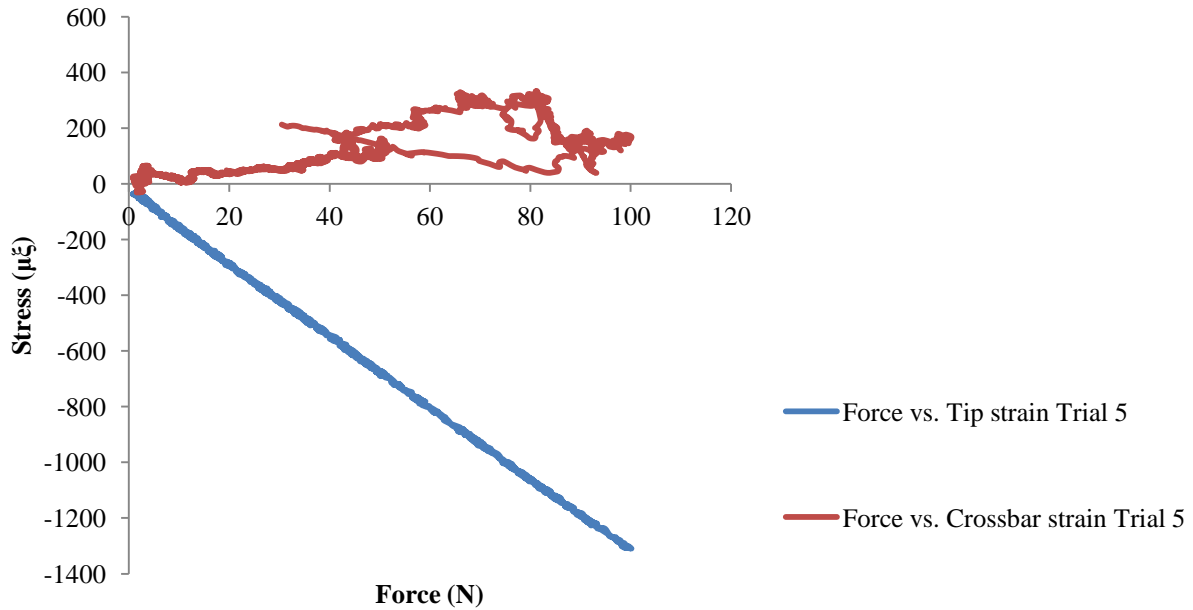


Figure 19. Graph of Force vs. Strain for Trial 5.

3.3 3D Modelling

In order to gain a visual representation of the two current models of Kerrisons at HSC, SolidWorks was used to do the 3D modeling. SolidWorks is a 3D CAD program which has several beneficial features. Each piece of the Kerrison can be modeled separately and then assembled at the end in order to make one finished fully movable product. FEA's can be conducted on individual parts or entire assemblies as will be explained in greater depth in section 5.2 of the report. Calipers and protractors were used to find the dimensions on the current and old Kerrisons in order to model them, while the future model was obtained through calculations. Dimensioned drawings can then be made from the 3D models in order to provide the information to manufacture the product.

3.4 Old Kerrison Model

The cross bar of the old model was the first part to be modeled. Extruded bases and splines were used to make the curvature of the crossbar. This version of the crossbar features the single keyway located closer to the cutting tip. Variable fillets were then used in order to give the smooth curves. This is illustrated in Figure 20.

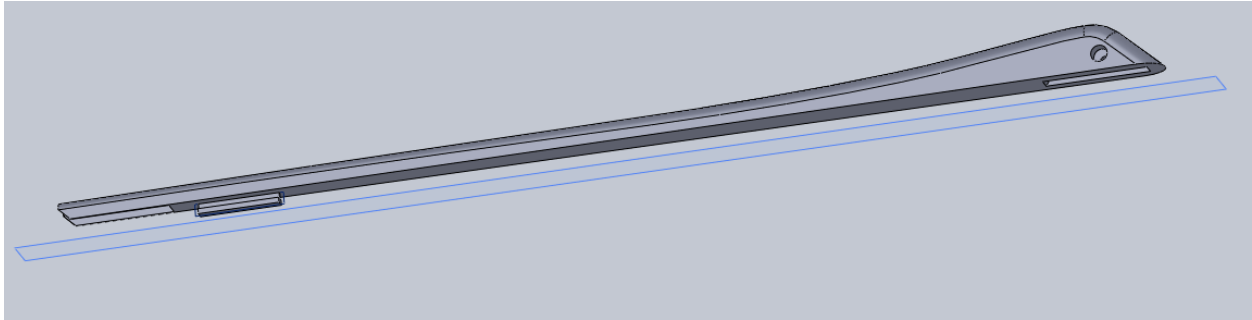


Figure 20. Non-detachable Kerrison crossbar.

The shank was then modeled with a flat smooth upper section for the crossbar to rest against. Hinge holes were lined up with those of the crossbar and where they will be located on the handles. Once again filleting was done to make smooth curves. This can be seen in Figure 21.



Figure 21. Non-detachable Kerrison shank.

The handle was a fairly simple design consisting of two holes where the handle will be hinged on the shank and the crossbar by screws. The grip of the handle was constructed using splines and variable fillets in order make the smooth curvature as seen in Figure 22.

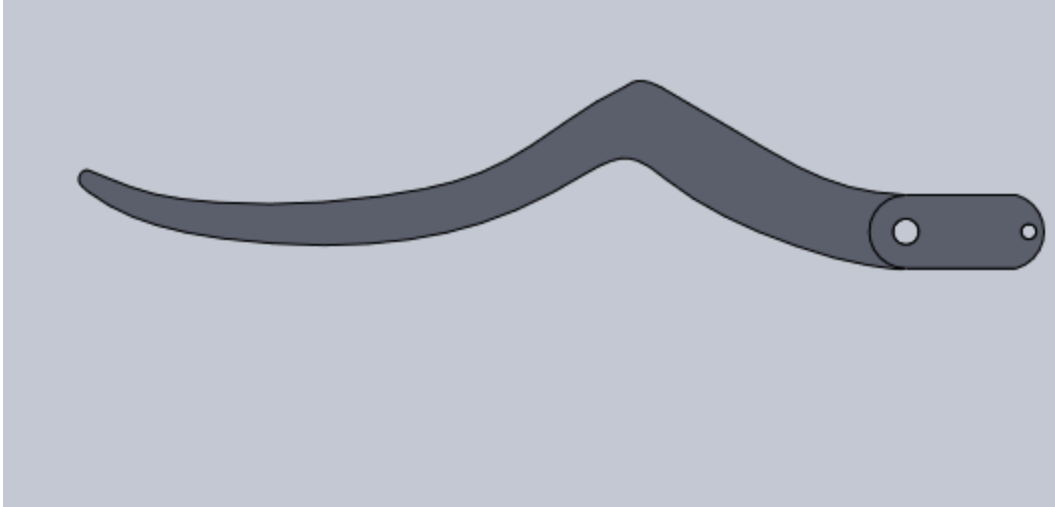


Figure 22. Non-detachable Kerrison handle.

3.5 Current Kerrison Model

The crossbar of the current detachable model required a few updates from the older non-detachable model. The keyway system was changed. As opposed to having one single keyway, a second keyway was added. One keyway fits inside the shank near the hinged screw and another keyway is located near the cutting edge outside the shank. These distinct features can be seen at point A and point B in Figure 23.

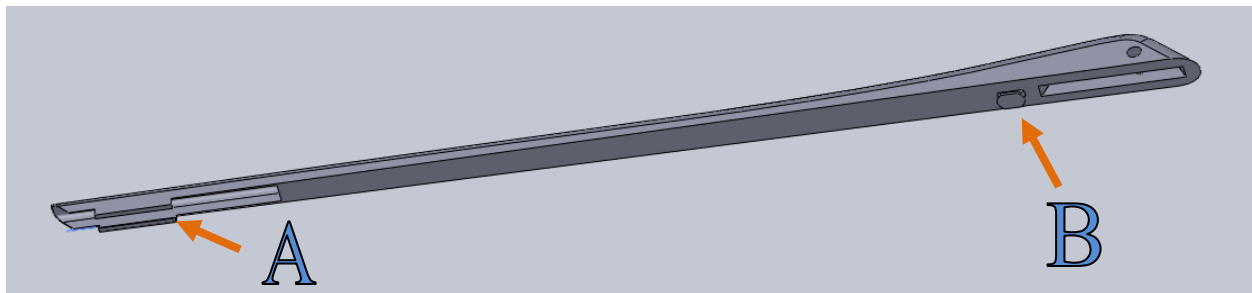


Figure 23. Adjustable Kerrison crossbar.

The shank needed to be altered in order to make the detachable model. Changes done to the crossbar needed to also be integrated to the shank. The slots for the keyway system described in the previous section needed to be added to the shank. An opening is added to the back of the shank above the hand rest to make room for the hammer. The changes are labeled in Figure 24.



Figure 24. Adjustable shank.

To allow for a detachable unit, the top half of the handle had to be completely redesigned. In order to maintain linear force transfer, the detachable models use a slot as opposed to hinge where the handle attaches to the crossbar. The overall geometry of the handle had to be altered as well to allow space for the hammer. Modifications are highlighted in Figure 25.

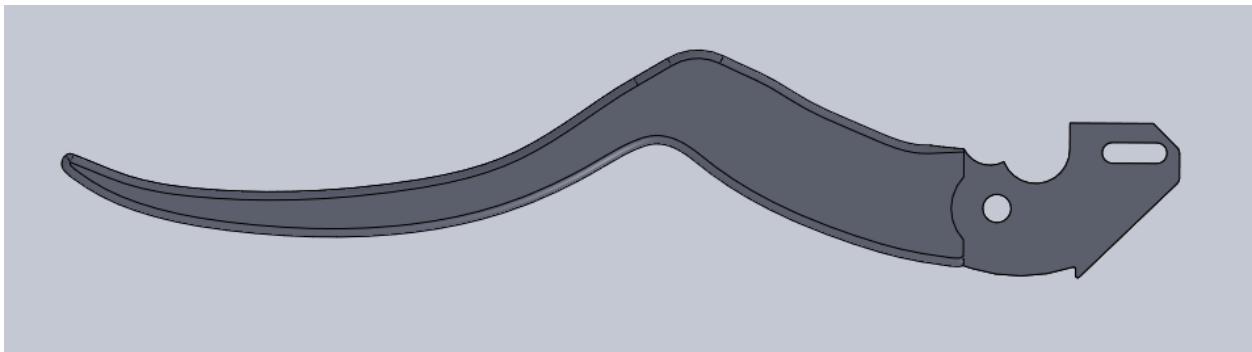


Figure 25. Adjustable handle.

3.6 Material Testing

The investigation into the bending failure of the cutting tip of the detachable Kerrisons and the search for a solution to the cutting tip failure, included an analysis of the material that the Kerrisons were composed of. Since no significant tip failure occurred on the older, non-detachable Kerrisons, the same material composition is acceptable as a benchmark for the redesigned Kerrison. The material used for the new Kerrison design is required to have material properties equal to or better than the non-detachable models from HSC. In order to recommend a material to use for the redesigned Kerrison, material analysis was required because the alloys and

coatings used by the manufacturers of such surgical tools are not disclosed for proprietary reasons.

It is also noted that only the non-detachable style of Kerrison was analyzed for material composition. The newer detachable model was not analysed due to the low availability of retired detachable Kerrisons. In order to carry out detailed material analysis, the tools were required to be destructively tested however this was not possible for the detachable Kerrisons currently in rotation at HSC. This limitation was of little consequence however, as the determined material would be set as the benchmark for the new Kerrison design.

With the material composition of the cutting tip as the focus of the material analysis, a sample of the 3 mm gold colored V. Mueller was taken from the tip of the hand rest. The material sample taken may be seen in Figure 26 and Figure 27. This sample was taken under the assumption that the base material and any coating at the hand rest would be identical to the base material and any coating present at the cutting tip. This assumption was made due to the fact that the Kerrison was assembled by 3 main components: the crossbar, the shank, and the handle. If the crossbar and the shank are made as a matching pair, they are likely machined from the same block of material, thus, having the same composition. Because the hand rest was located on the shank, it was assumed that it would be made of the same material as the cutting tip, making the hand rest an appropriate place to take a material sample. Additionally, any coating that would be present was assumed to be the same for the hand rest and the cutting tip because of the uniform color, due to physical vapor deposition of the coating, on the Kerrison.

The initial hypothesis for material composition of the Kerrison was some kind of stainless steel for the base material, with a coating of Titanium Nitride.



Figure 26. V. Mueller Kerrison with material sample cuts.



Figure 27. V. Mueller Kerrison with samples removed.

The sample taken from the V. Mueller Kerrison was cut once more to expose a cross section of the tool for one sample as seen in Figure 28, and to expose the outer surface of the tool as seen in Figure 29.



Figure 28. V. Mueller Kerrison cross sectional sample.



Figure 29. V. Mueller Kerrison surface sample.

Material analysis was performed using a scanning electron microscope (SEM) and was able to determine the chemical composition of the Kerrison using energy displacement spectroscopy (EDS). The images produced by the SEM were produced by observing elastic and inelastic collisions between electrons, while the chemical composition of the material was determined by the energy levels of the x-rays that were emitted from the electron collisions. However, the particular software suite that was utilized to perform the material analyses imposed a limit to the

analysis in the unreliable measurement of lighter elements such as Carbon, Nitrogen and Oxygen. Because of the low certainty of the amount of such light elements, the weight percentages listed in the tests must be taken with a grain of salt. The weight percentage measurements of the heavier elements were influenced if a lighter element was selected to be measured by the software, however if only metals were selected to be measured by the software, the weight percentage measurements were taken to be precise.

SEM testing was done on two separate occasions. The first session was on November 8th 2011 and the second was on November 18th 2011. The results from the tests are as follows:

TABLE I SESSION 1 CROSS SECTION ANALYSIS

Trial 1		Trial 2		Trial 3		Trial 4	
Element	Wt. %						
C	13.47	-	-	-	-	-	-
Si	0.55	Si	0.69	Si	0.69	Si	0.69
Cr	11.96	Cr	13.76	Cr	13.75	Cr	13.75
Fe	70.38	Fe	81.31	Fe	81.2	Fe	81.2
Co	0.2	Co	0.23	Co	0.23	Co	0.23
Ni	0.25	Ni	0.3	Ni	0.3	Ni	0.3
Cu	3.2	Cu	3.73	Cu	3.73	Cu	3.73
Re	-0.02	Re	-0.03	Re	-0.03	Re	-0.04
-	-	-	-	Mo	0.13	Mo	0.12
-	-	-	-	-	-	Ti	-0.07
-	-	-	-	-	-	Zr	0.09

TABLE II SESSION 1 SURFACE ANALYSIS

Trial 1		Trial 2	
Element	Wt. %	Element	Wt. %
Ti	18.87	Ti	14.6
Cr	0.85	Cr	0.66
Fe	3.95	Fe	3.14
Co	0.03	Co	0.02
Ni	0.17	Ni	0.13
Cu	0.09	Cu	0.07
Zr	76.1	Zr	59.28
Mo	-0.04	Mo	-0.03
-	-	N	22.12

TABLE I and TABLE II show the difference in material between the cross section and the surface, and confirm the initial hypotheses. The high percentage amounts of Iron along with significant amounts of Chromium for all trials in TABLE I indicate a stainless steel of some kind. The material composition of the surface of the sample shown in TABLE II is very different. Titanium makes up a significant portion in both Trials with Zirconium having the majority of the surface composition while both Iron and Chromium are significantly lower in weight percentage. This difference between the cross section and surface composition indicates that a surface coating is indeed present on the Kerrison. The measurement of light elements is seen to be unreliable as the inclusion of Carbon for the first Trial in TABLE I shows a measurement of 13.47 weight percentage, which is an unreasonably high amount of carbon for any stainless steel. Most stainless steels have carbon compositions well below one percent. Trials 2 through 4 show more reliable results, with little variation in weight composition when additional heavy elements are considered. Trial 2 in TABLE II also shows unreliable measurement of light elements with inconsistency in weight percentage composition when Nitrogen is included. Titanium Nitride (TiN) and Zirconium Nitride (ZrN) are strong candidates for the coating material, however it was impossible to pin point the exact material without a reliable measurement of Nitrogen. Figure 30 through Figure 33 show the electron microscope

photographs of the samples that were analyzed as well as the spectrum of elements that were included in the weight percentage compositions.

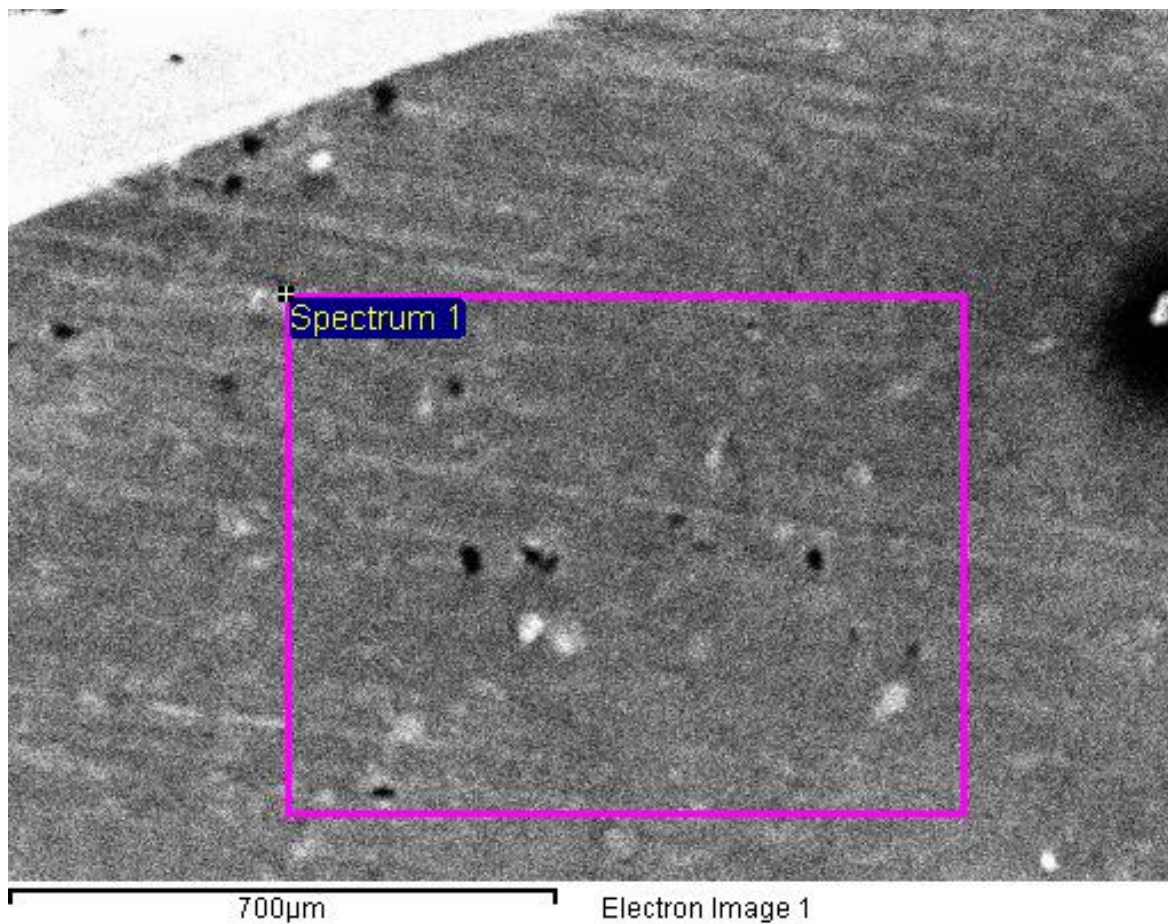


Figure 30. Scanning electron microscope photograph of Kerrison cross section.

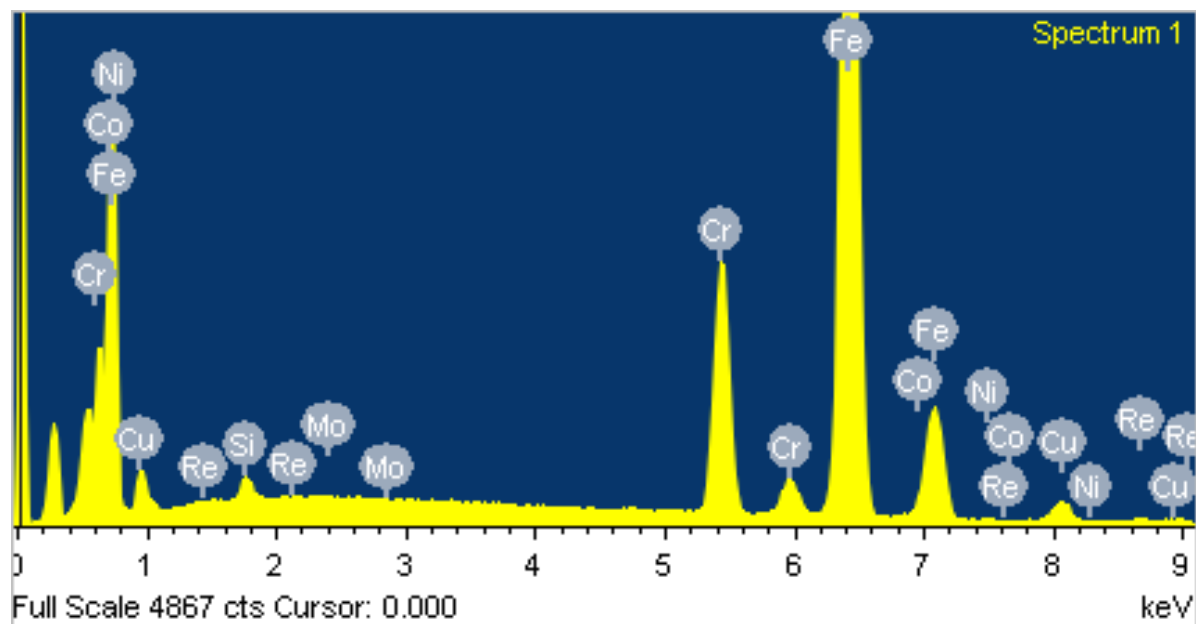


Figure 31. Session 1 Kerrison cross section Trial 3 material analysis spectrum.



Figure 32. Scanning electron microscope photograph of Kerrison coating.

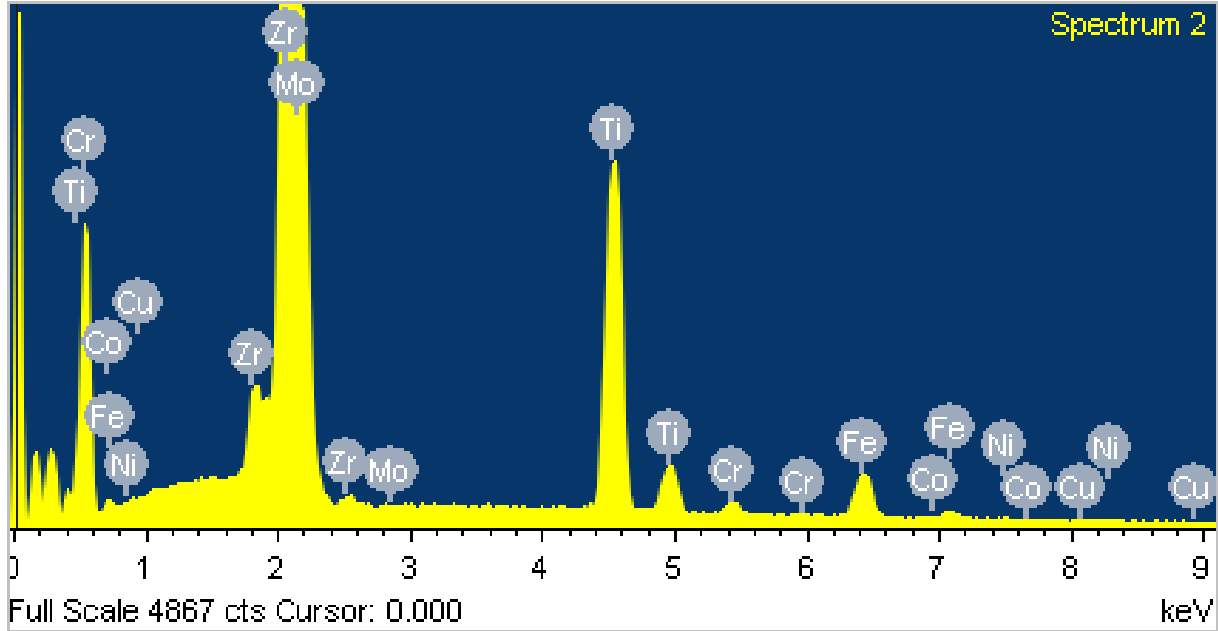


Figure 33. Session 1 Kerrison coating Trial 1 material analysis spectrum.

TABLE III SESSION 2 CROSS SECTION ANALYSIS

Trial 1		Trial 2		Trial 3	
Element	Wt. %	Element	Wt. %	Element	Wt. %
C	18.81	N	1.05	O	1.24
Al	-0.04	Al	-0.05	Al	-0.05
Si	0.38	Si	0.52	Si	0.52
Cr	12.17	Cr	14.74	Cr	14.71
Fe	67.94	Fe	82.77	Fe	82.6
Ni	0.13	Ni	0.16	Ni	0.16
Mo	0.08	Mo	0.11	Mo	0.1
Ta	0.29	Ta	0.39	Ta	0.39
W	0.24	W	0.32	W	0.32

TABLE IV SESSION 2 SURFACE ANALYSIS

Trial 1		Trial 2		Trial 3		Trial 4		Trial 5		Trial 6	
Element	Wt. %										
C	25.08	N	19.2	O	29.87	C	23.27	N	21.57	O	32.96
Al	0.05	Al	0.04								
Ti	11.57	Ti	12.35	Ti	10.44	Ti	11.4	Ti	11.51	Ti	9.55
Cr	0.25	Cr	0.26	Cr	0.22	Cr	0.26	Cr	0.26	Cr	0.22
Fe	1.51	Fe	1.59	Fe	1.36	Fe	1.41	Fe	1.41	Fe	1.19
Ni	-0.03	Ni	-0.04	Ni	-0.03	Ni	-0.06	Ni	-0.06	Ni	-0.05
Cu	-0.02	Cu	-0.02	Cu	-0.02	-	-	-	-	-	-
Zr	60.94	Zr	65.91	Zr	57.51	Zr	63.64	Zr	65.23	Zr	56.07
Nb	1.69	Nb	1.82	Nb	1.58	Nb	1.31	Nb	1.34	Nb	1.15
Mo	-0.1	Mo	-0.11	Mo	-0.09	Mo	-0.08	Mo	-0.09	Mo	-0.07
Ta	-0.77	Ta	-0.84	Ta	-0.74	Ta	-1.07	Ta	-1.1	Ta	-0.96
W	-0.17	W	-0.18	W	-0.16	W	-0.12	W	-0.12	W	-0.11

The second session of material analysis of the cross section and surface sample using the SEM and EDS considered measurements of Carbon, Nitrogen and Oxygen along with the heavier metal elements. Any conclusions regarding the actual material used for the Kerrison drawn from the material analysis that includes the lighter elements would be inaccurate; however other tests performed during session two highlight the presence of a coating over a base material, as well as a certain gradient of material composition through the coating.

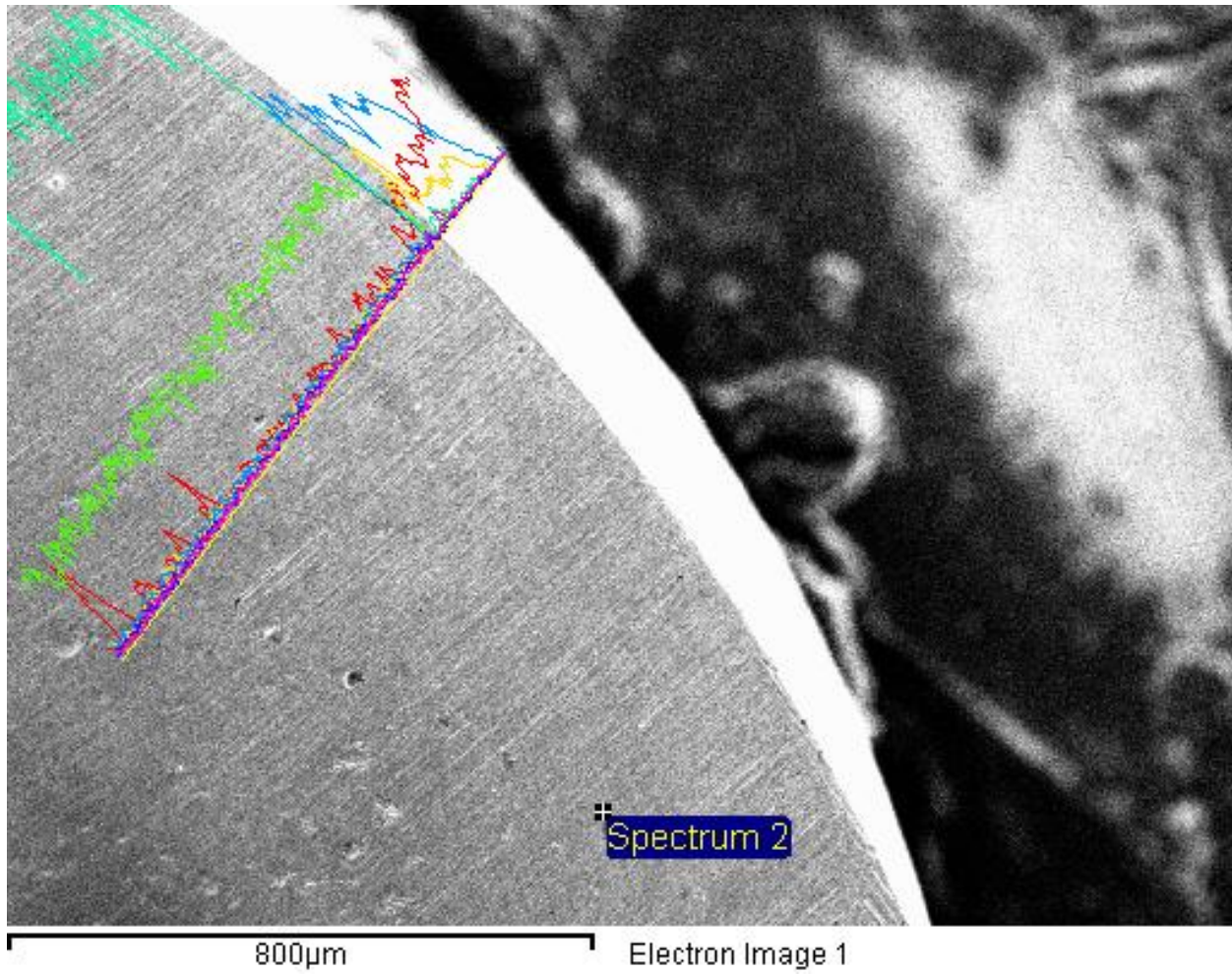


Figure 34. SEM photograph of material with composition analysis going from cross section to coating.

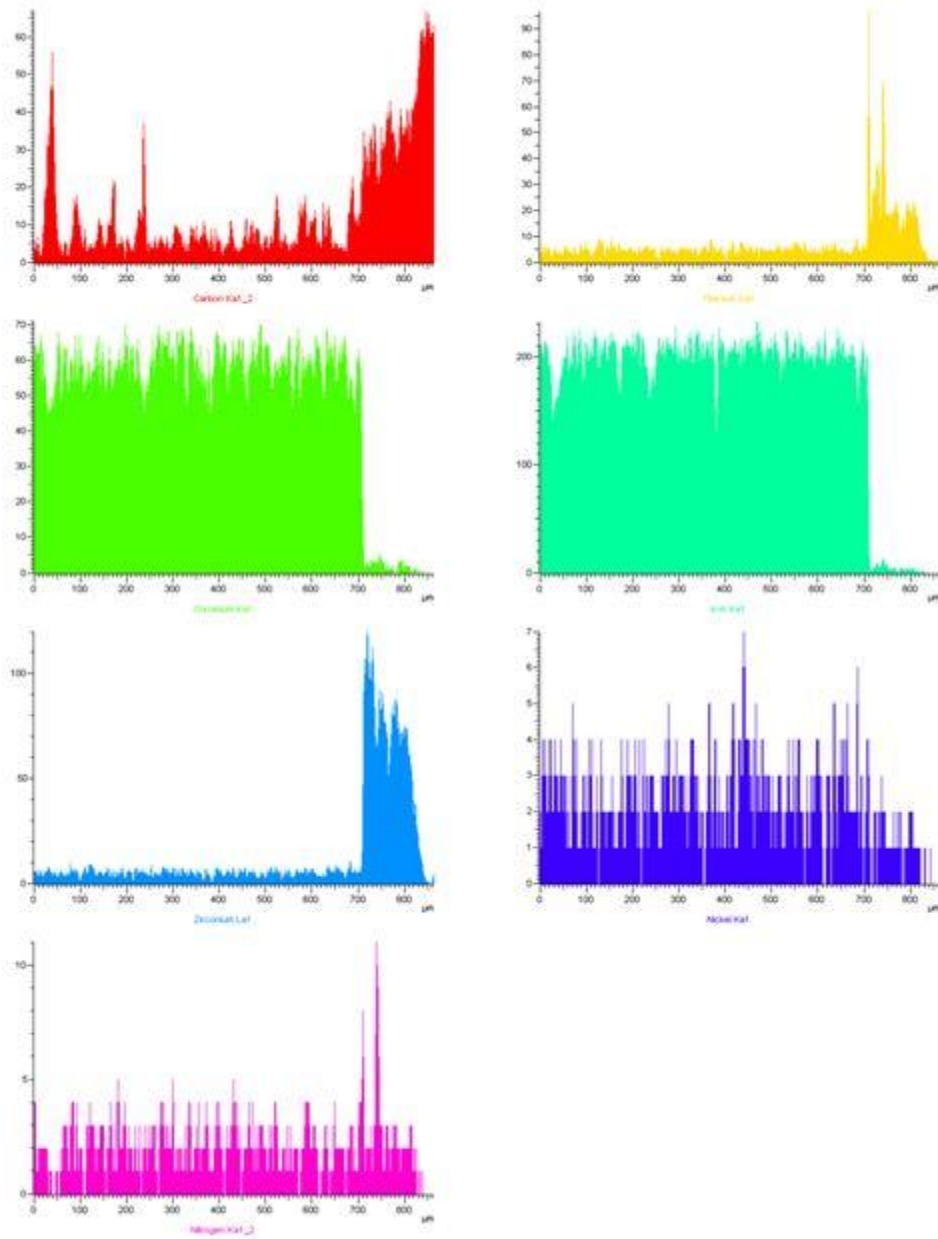


Figure 35. Element presence going from cross section to coating.

TABLE V COLOR KEY FOR ELEMENT PRESENCE GOING FROM CROSS SECTION TO COATING

Color	Element
Red	Carbon
Yellow	Titanium
Green (on left)	Chromium
Green (on right)	Iron
Blue	Zirconium
Purple	Nickel
Pink	Nitrogen

Figure 34 shows the motion of the electron beam across the cross section face and the location of the measurement along with the color coded elemental presence. As the SEM moves across the face of the cross section and into a cross sectional area where the coating is present, the changes in the elements present are significant. The dark grey section is the stainless steel interior material and the white edge is the coating.

Figure 34 and Figure 35 show that inside the grey portion of the cross section, Chromium and Iron are abundant, along with some presence of Nickel. These three elements then reduce significantly sharply while at the same Titanium, Zirconium and Nitrogen sharply increase in presence. The corresponding rise and fall of elements again confirm the presence of a base material that is some kind of stainless steel and a coating that is composed of Titanium, Zirconium and Nitrogen. The measurement of Carbon, shown as a red graph in Figure 35, is full of noise and difficult to read anything of significance from. One interesting thing to note from Figure 35 is the varying amounts of Titanium and Zirconium inside the coating region. This variation of material may be attributed to multiple layers of TiN and ZrN coating that have been applied on top of each other.

Considering the elements chosen and the impact of the inclusion of light elements, the cross section analysis of trial 3 from section 1, shown in TABLE I, was chosen to match the chemical composition to an existing known alloy. This trial had measured weight percentage compositions of Si at 0.69%, Cr at 13.75%, Fe at 81.2 %, Co at 0.23%, Ni at 0.3%, Cu at 3.73%, and Mo at 0.13%. After consultation with various sources it was determined that the material of the V.

Mueller Kerrison was a 400 series martensitic stainless steel [4], [5]. The 400 series stainless steels have excellent mechanical properties and contribute to the resistance of tip deformation during the non-detachable Kerrison's cutting motion.

Through help from the UofM materials lab, SEM analysis was able to identify the chemical composition of the Kerrison surface coating and base material, however it must be noted that detailed grain structure analysis was not performed due to limitations on the resources and technical lab staff available. To observe the microstructure of the material and look at grain orientation through the cross section of the material, much processing would have been required by skilled technicians to properly capture, mount, polish and etch a suitable sample. Detailed study of the grain structure would have shed light on any additional processing of the tool to make it stronger, such as heat treatments that may have been performed, or case hardening to strengthen the outside of the tool. However, because this detailed grain analysis was not performed, any possible treatments such as these that may have occurred on the old style non-detachable Kerrison were unknown.

3.7 Factors not considered

There are some topics that were not extensively studied in this report that may have been considered as factors that could lead to failure. The following is a list of topics that to some degree may have led to failure, but were not discussed due to a variety of reasons. We will discuss briefly what the topic was, and why we chose not to test further.

3.7.1 Foot Plate Deformation:

The foot plate or (anvil) shown as Detail G in Figure 1 acts as a cutting surface that holds the material in place while the tip slices it away. Size restrictions limited our ability to conduct physical testing such as strain gage analysis. It was found in our research that the foot plate was able to distribute the load more effectively than the cutting tip due to its geometry. Since the cutting tip focused the majority of its cutting force on the sharp pointed tip, it became much more susceptible to deformation than the footplate. This resulted in very low footplate deformation when compared to the cutting tip. We have concluded that the cutting tip of the crossbar will deform much sooner than any deformation of the footplate, and we can therefore neglect any further experimentation on the foot plate.

3.7.2 Torque and twisting:

During surgery, the Kerrison experiences significant twisting and tugging when biting away tissue and bone. In our discussions with two different surgeons who use the tool on a daily basis, they stated that the need for twisting and tugging was reduced when the Kerrison tip was sharp, and increased as the tip dulled. Due to time and size restrictions, we were unable to run physical experimentation on the Kerrison to prove these statements. We believe that by implementing measures discussed previously in the report to keep the tip sharp for longer periods of time, the amount of twisting will be reduced, decreasing the amount of deformation.

3.7.3 Biting of tissue:

Tissue is much softer and less damaging to bite into than bone or cartilage. Seeing as we plan on testing the Kerrison to the worst case scenario we decided to assume the cutting of bone rather than tissue during testing. Biting tissue becomes a problem when using a dull Kerrison tip, and as discussed previously, we will be implementing methods that will keep the cutting tip sharper for longer, reducing this problem.

4 Redesign of Kerrison Rongeur

4.1 Overview

The following is a list of the alterations and additions that were made to the original Kerrison during the redesign process:

- Slot drive for the force transfer mechanism
- Staged sharpening with multiple handles
- Hand rest
- New choices for material and coating selection

These alterations are shown below in Figure 36.

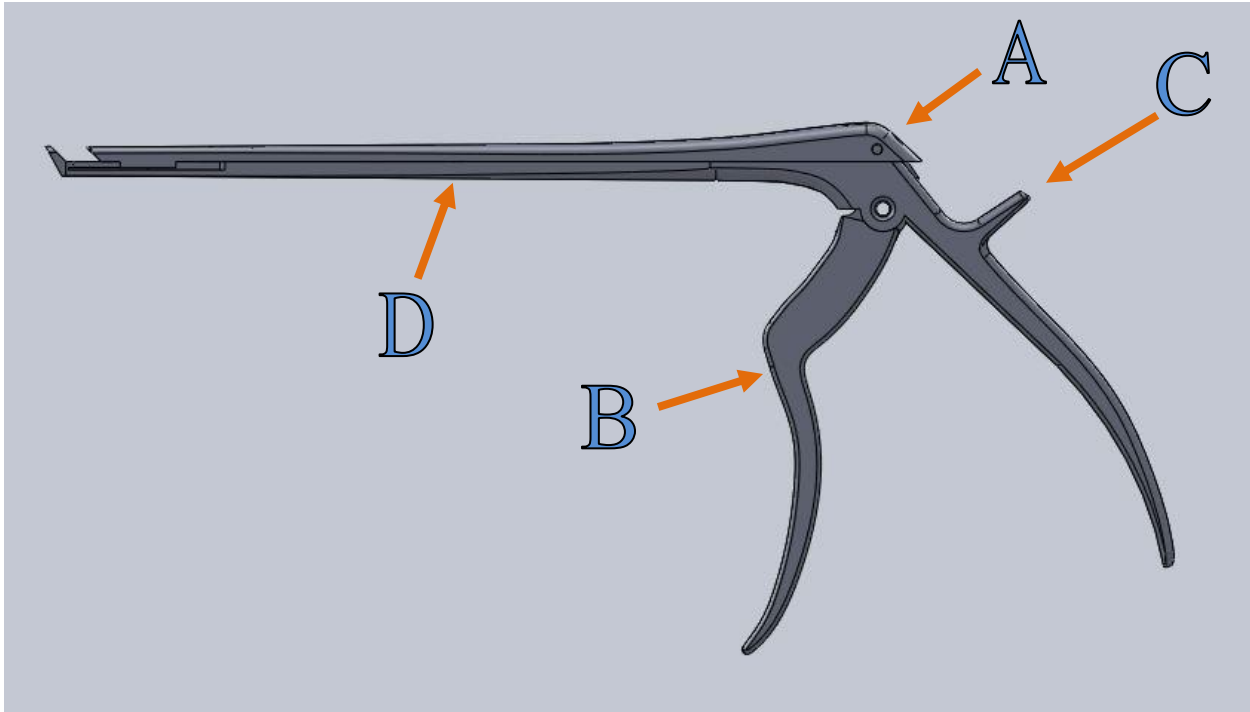


Figure 36. Overview of redesigned Kerrison.

Our client decided that the various features from our patents and competitor products searches are not to be considered for implementation. Inclusion of any such features would pose the risk of infringement on the existing patents. For simplicity, our client decided that the final design should remain as geometrically similar as possible to the current Kerrisons in use by surgical staff at HSC.

Details regarding each redesigned feature will be discussed further in the following sections.

4.2 Handle Redesign

The Kerrison handles exhibit two important redesign characteristics: slot drives (A) for the transfer of force along the crossbar and multiple handles (B) to accommodate stage sharpenings.

4.2.1 Linear Transfer Mechanism

It has been previously noted that a prominent problem with several of the current Kerrisons is the bowing of the crossbar during the application of force by the hand. This effect has been found to cause significant transverse deflections near the center of the crossbar, resulting in a slight gap between the crossbar and the shank. This gap can subsequently hinder the efficiency of force transfer along the crossbar.

The bowing effect is partially a result of the pin joint used in several of the current instruments. An example of this linear transfer mechanism is shown below for the current non-detachable Kerrison model in Figure 37.

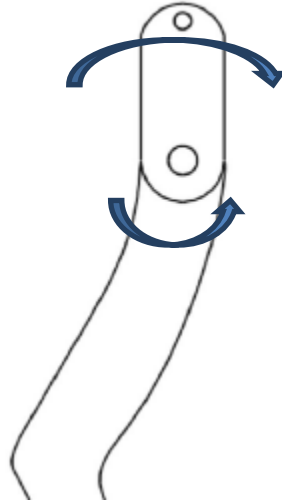


Figure 37. Force transfer mechanism of non-detachable model.

Several current instruments utilize a slot drive instead of a pin joint. The slot drive allows for an improved linear motion since the handle pin is allowed to move horizontally without being constrained by following a curved path. Figure 38 depicts this slot drive mechanism.

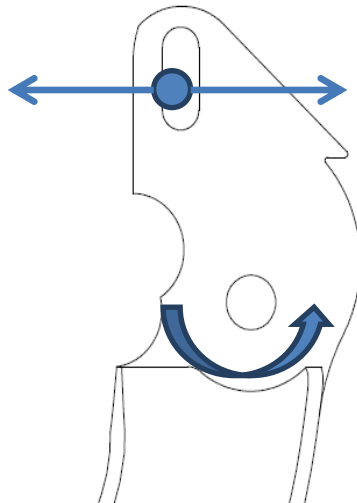


Figure 38. Force transfer mechanism of detachable model.

4.2.2 Staged Sharpening with Multiple Handles

In order to improve the service life of each Kerrison, the cutting blade can be sharpened after several surgeries in preparation for future operations. The surgical instrument technician currently performs sharpening on the cutting tips of the Kerrisons in use. The tip is generally sharpened by a length of approximately 20 to 30 thousandths of an inch (approximately 1/32") each time. However, the current Kerrisons are only able to be sharpened by small amounts before the crossbar would become insufficient in length to reach the anvil during the cutting action.

Our solution to this problem is simple: the implementation of multiple handles for each instrument allows each handle to possess varying geometries and locations of the slots. This in turn allows for each handle to accommodate different stages of sharpening. The first stage would be geometrically identical to the handle of the current detachable Kerrison. Subsequent stages would comprise altered slot geometry, where the slot would be translated forward and upwards on the handle. Figure 39 depicts the current handle design followed by two subsequent sharpening stages.

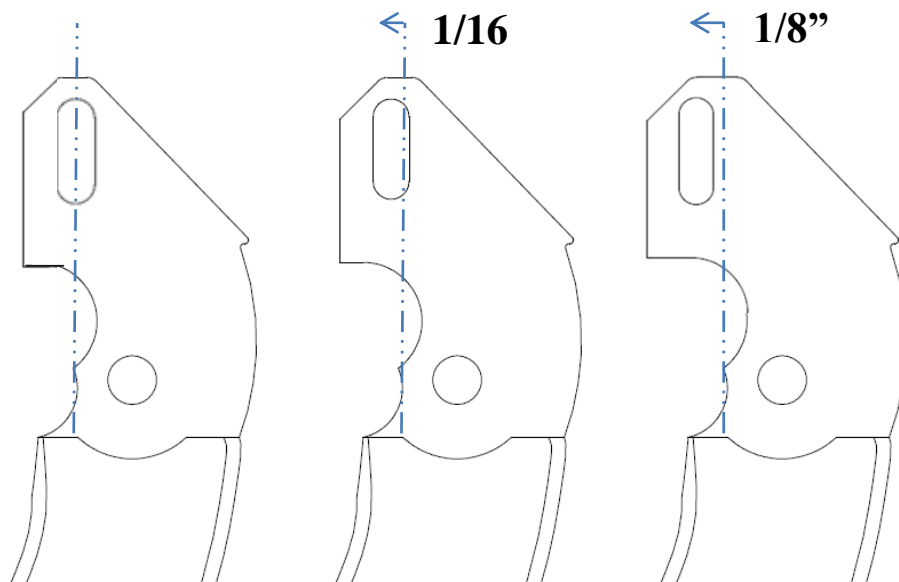


Figure 39. Designs for three stages of staged sharpening concept.

Once the blade has been sharpened back at least 1/16” then the next stage would need to be implemented. This would simply involve replacing the first handle with the second stage handle, which comprises the altered slot geometry. The second stage would ideally allow for a further 1/16” of sharpening before the third stage would be required, and the process could be repeated.

4.3 Hand Rest Redesign

The importance of ergonomics in the design of a Kerrison can be easy to overlook. A lot of focus and calculations are put into determining the forces, stresses and strains that the unit will withstand, but all of this would be for not if the tool is not comfortable to use. During our visit to HSC, observation of surgery, and discussion with the surgeons and staff, it was brought to our attention just how important the factor of ergonomics is. We learned that several fundamentally and technically sound instruments are brought in and no matter how effective they are, the surgeons would refuse to use them if they were not comfortable. During a discussion with a surgeon it was brought to light that when the Kerrisons are being passed from nurse to surgeon they find themselves getting poked and prodded in the palms by the hand rest. The hand rest on the current models stick out almost horizontally from the handle and are not very smoothed at the tip as can be seen in Figure 40 below.



Figure 40. Hand rest of current Kerrison models.

This conversation spurred the idea to have the hand rest redesigned. Removing the hand rest would completely remove the inconvenience of getting poked by the instrument; however, with no hand rest it would very difficult to apply the full force of your squeeze without somewhere to anchor your hand. When squeezing on the handle, especially if the Kerrison is angled, the hand has a tendency to slide. The hand rest is installed in order to secure your hand in position while you make the cut. A new design for this part was generated that will not only greatly reduce the frequency at which the jamming might occur, but will also provide a more comfortable place to rest your hand. The new design features a rounded out hand rest, as seen in point A of Figure 41.

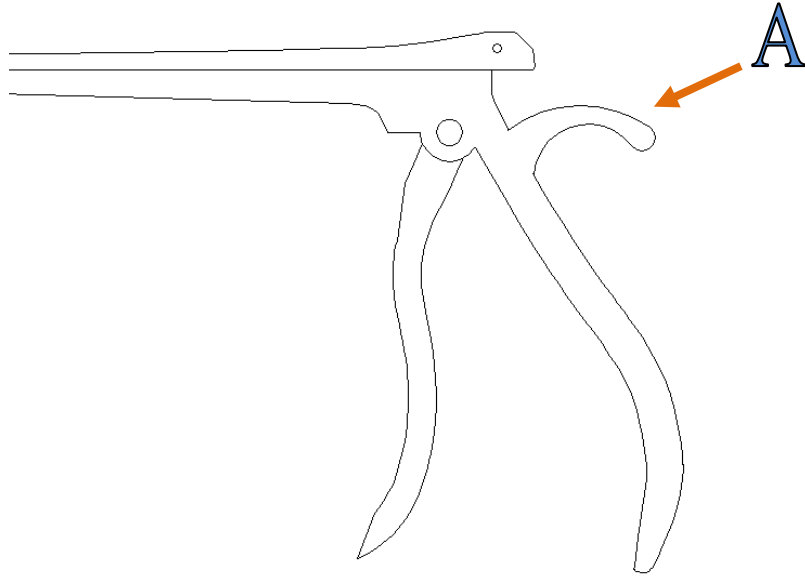


Figure 41. Redesigned hand rest.

This feature would not add any total cost to the unit as we are simply reshaping the current hand stop to a more ergonomic shape.

4.4 Blade Height Reduction

When the detachable Kerrisons at HSC first started experiencing unacceptable tip deformation, the increased height of the detachable Kerrison's tip over the non-detachable tip was suspected to be a contributing factor in the cause of deformation. The difference in Kerrison bite heights is shown in Figure 42. All three cuts in the paper are made by a full bite of a Kerrison, each of a different make. The cuts on the left and in the middle, labelled Jarit and Ruggles, were made by newer detachable models while the cut on the right was made by the established non-detachable Mueller Kerrison. Both cuts made by the detachable models are taller in height than the non-detachable model. The correlation of the taller bite height with the deformation experienced by the detachable model's tips along with the shorter bite height with the lack of deformation by the non-detachable model's tips led to the thought that the taller bite height could contribute to tip deformation.

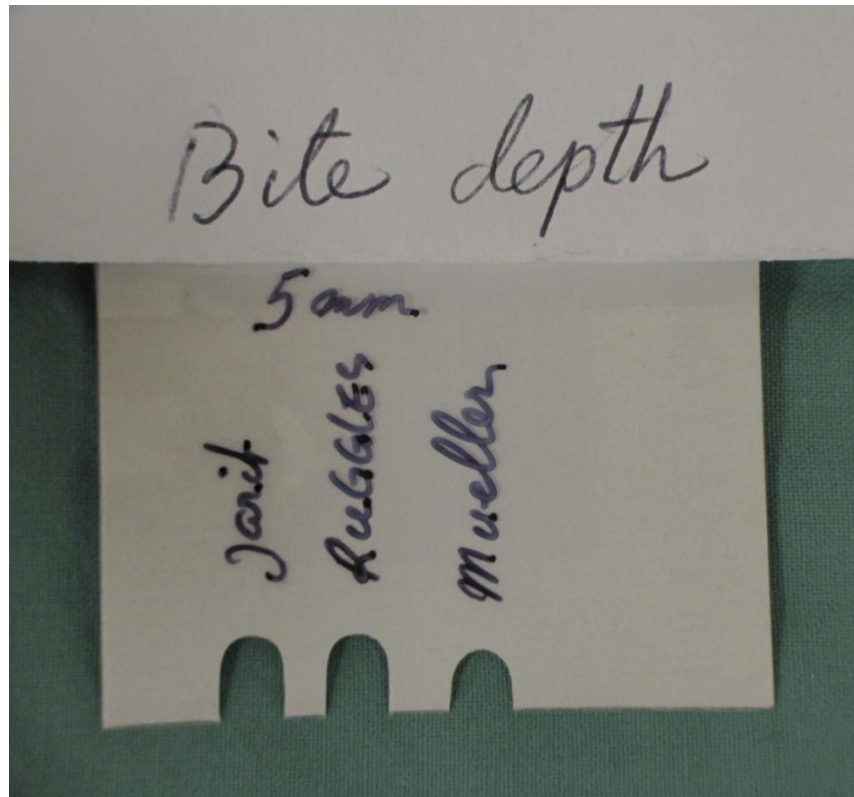


Figure 42. Kerrison bite height comparison, used with permission [3].

This hypothesis was tested by performing FEA on Kerrison crossbars with four different bite heights of 3.5 mm, 3.0 mm, 2.5 mm and 2.0 mm and are shown in Figure 43 through Figure 46.

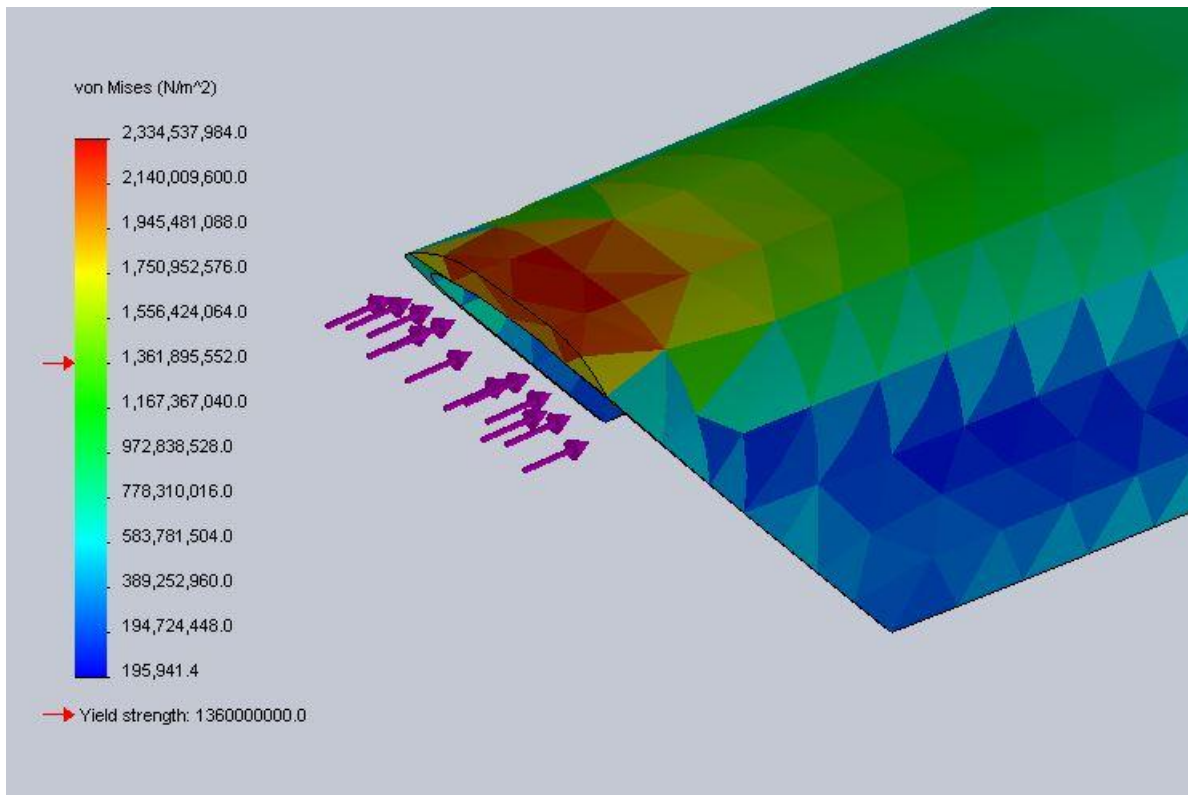


Figure 43. FEA of cutting tip with 3.5 mm bite height.

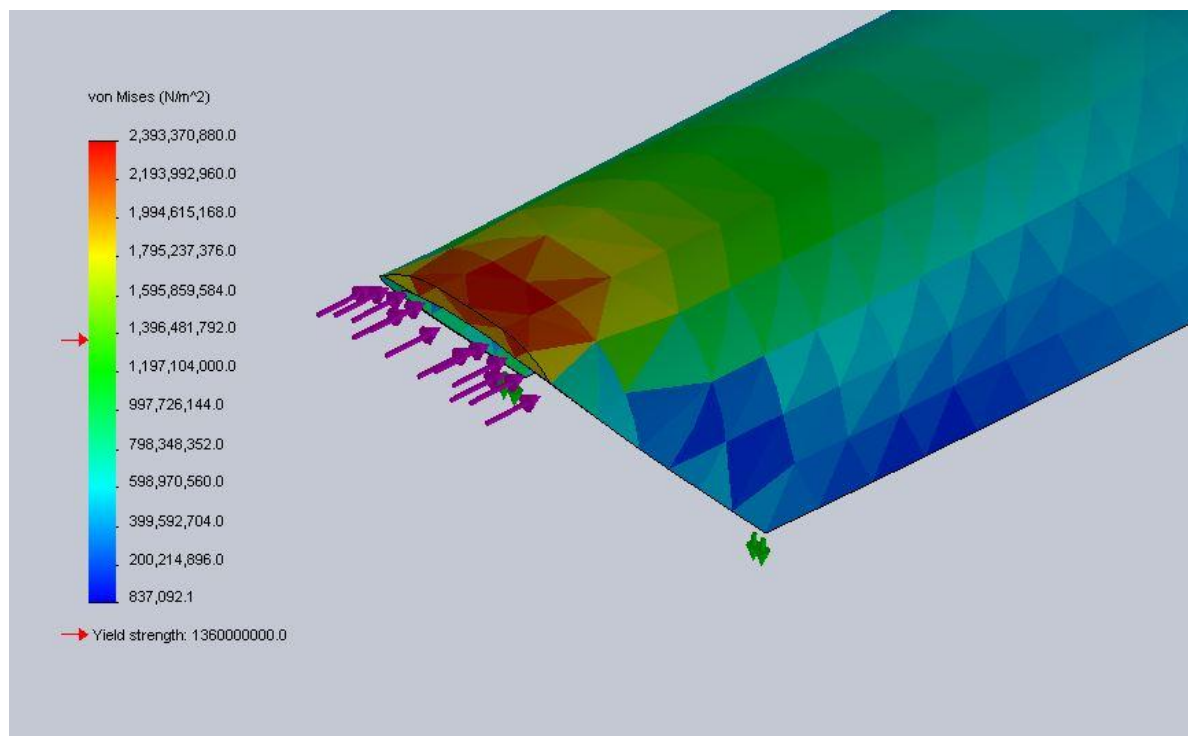


Figure 44. FEA of cutting tip with 3.0 mm bite height.

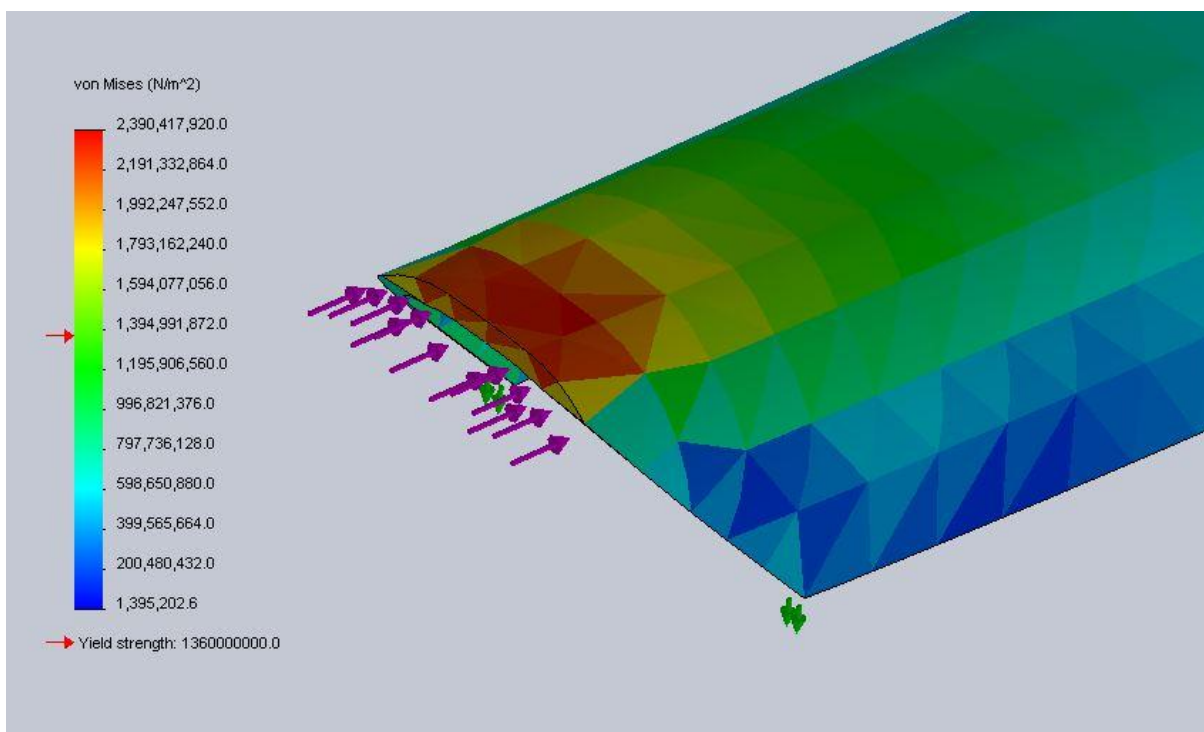


Figure 45. FEA of cutting tip with 2.5 mm bite height.

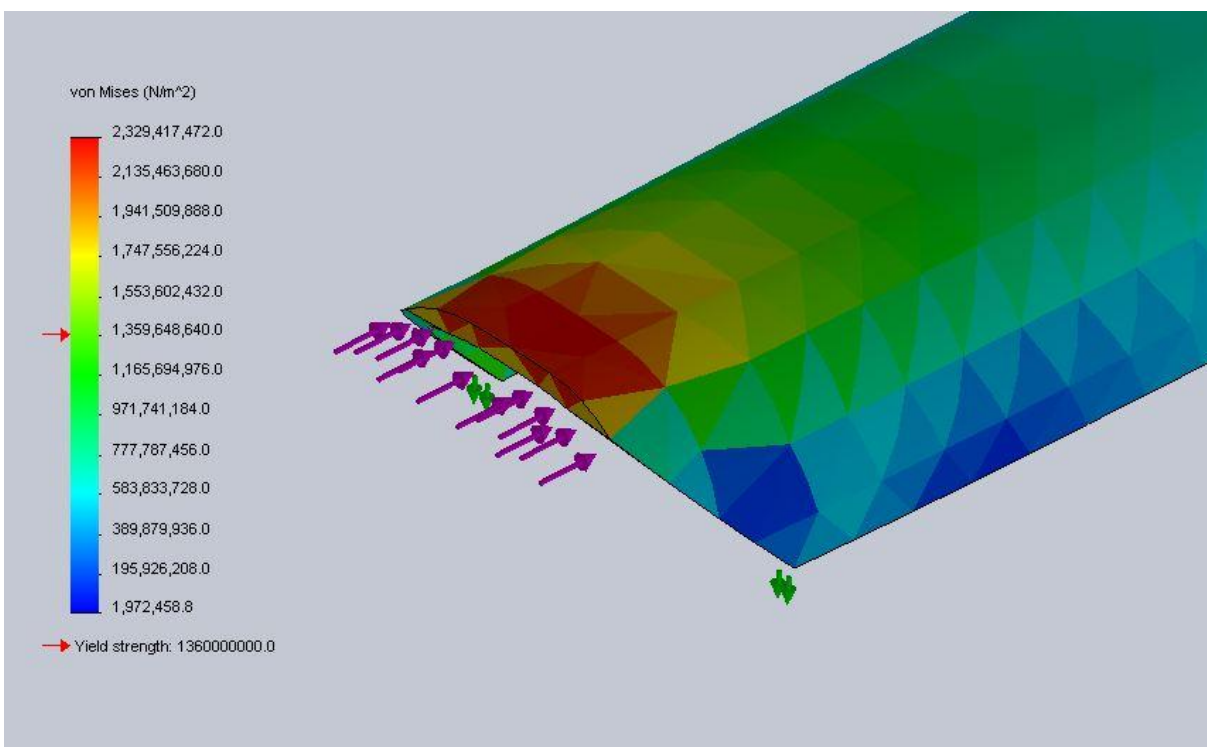


Figure 46. FEA of cutting tip with 2.0 mm bite height.

The loading situation simulated a cut made by the very top of the tip in order to place the force on the smallest area possible to find maximum levels of stress in tip. This loading also simulates many of the cuts that would be made during an operation where fine cuts and small amounts of bone material are to be removed. A 1000 N load was applied to the tip, a load which was experimentally measured to be the maximum amount of force the Kerrison would be able to supply when operated by a strong human hand.

In every FEA experiment the tip failed and deformed, with the stresses exceeding the yield stress of the specified material properties for the experiment. Despite failure for every tip height that was tested, significant reduction in the maximum stresses experienced in the cutting tip was not realized as the tip height was reduced. The tip height reduction study is summarized in TABLE VI.

TABLE VI TIP HEIGHT REDUCTION COMPARISON

Tip Height [mm]	Maximum Stress [GPa]	Change in Stress from 3.5 mm
3.5	2.334	-
3.0	2.393	2.5%
2.5	2.390	2.3%
2.0	2.329	-0.2%

The stress experienced in the 3.5 mm tall tip was actually lower than the 3.0 mm and 2.5 mm tall tips. There was a slight reduction in the maximum stress as the tip height moved from 3.0 mm down to 2.0 mm, however the stress reduction was nearly insignificant, and not nearly as significant as the reduction in cutting capacity that the tool would experience as the tip height would move from 3.5 mm down to 2.0 mm.

As a result of the FEA study and the lack of maximum stress reduction due to the reduction of the tip height, the tip height reduction concept for the redesigned Kerrison was not to be pursued any further, and is not recommended.

4.5 Material and Coating Selection

Considering the 400 series of stainless steels as the material used in the non-detachable Kerrison and taking that material as a benchmark for the new material to be used in the redesigned Kerrison, the material chosen for the new Kerrison would ideally have slightly better physical properties in terms of ultimate strength, yield strength and corrosion resistance. TABLE VII lists

critical physical properties of the commonly used, and most likely the actual material for the non-detachable Kerrison, 410 martensitic stainless steel along with the 420 martensitic stainless steel.

TABLE VII 410 AND 420 MARTENSITIC STAINLESS STEEL PROPERTIES [5], [6]

Mechanical Property	410 Stainless Steel	420 Stainless Steel
Density	7.80 g/cc	7.80 g/cc
Hardness, Rockwell C	45	57
Ultimate Tensile Strength	1525 MPa	2025 MPa
Yield Tensile Strength	1225 MPa	1360 MPa
Elongation at Break	14.5%	2.50%
Reduction of Area	45.0%	-
Modulus of Elasticity	200 GPa	200 GPa
Poisson's Ratio	-	0.240
Shear Modulus	-	80.7 GPa

The stainless steel recommended for the Kerrison redesign is the 420 martensitic stainless steel. “Grade 420 stainless steel is a higher carbon version of 410; like most non-stainless steels it can be hardened by heat treatment. It contains a minimum of 12 per cent chromium, just sufficient to give corrosion resistance properties. It has good ductility in the annealed condition but is capable of being hardened up to Rockwell Hardness 50HRC, the highest hardness of the 12 per cent chromium grades. Its best corrosion resistance is achieved when the metal is hardened and surface ground or polished” [7]. A 420 stainless steel containing Molybdenum should be used to maintain high hardness and strength while the Molybdenum increases corrosion resistance to prolong tool life throughout the cleaning cycle for surgical tools at HSC.

The coating of the V. Mueller was observed to be composed of Titanium, Zirconium and likely Nitrogen. While the exact order and location of the coating layers and elements was not able to be determined, a scheme of alternating layers of TiN and ZrN coatings would contribute to the hardness, biocompatibility and corrosion resistance of the Kerrison [8].

5 Analysis of Redesigned Kerrison

5.1 3D Modeling

Due to an increase in the size of the handles, the curvature of the crossbar had to be increased in order to avoid friction between the crossbar and the handle while it is in motion shown in Figure 47.

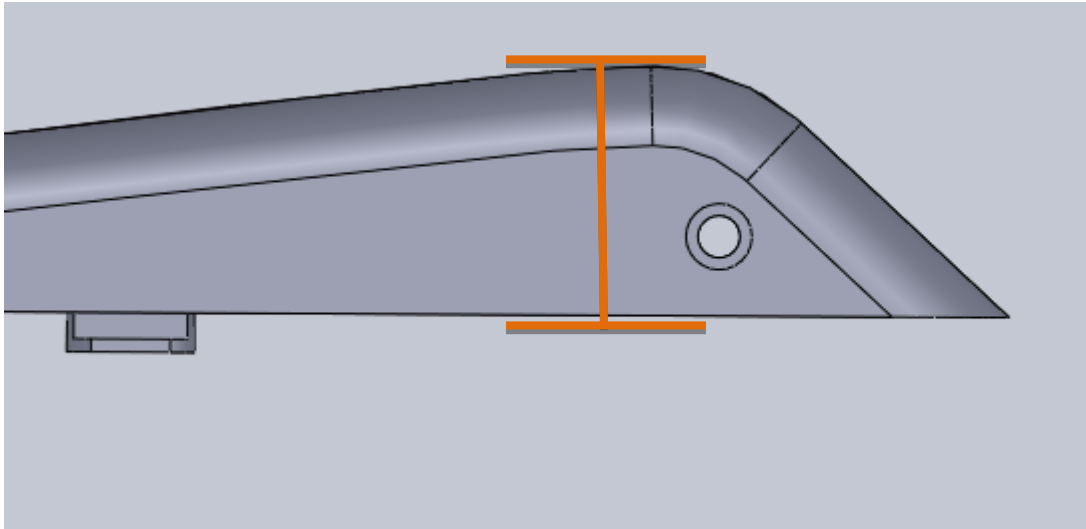


Figure 47. New crossbar height.

Figure 48 shows the future model of the shank incorporates the newly designed hand rest that has a curved surface as well as smoothed off tip in order to increase ergonomics of the Kerrison.

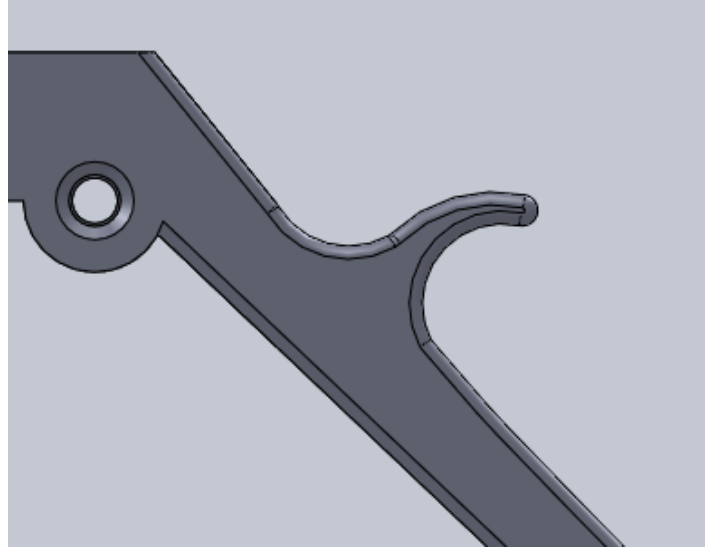


Figure 48. Curved Hand Rest.

Three handles needed to be designed for the future model, as discussed previously in section 4.2.2. Figure 49 below depicts computer models of the three stages of handles.

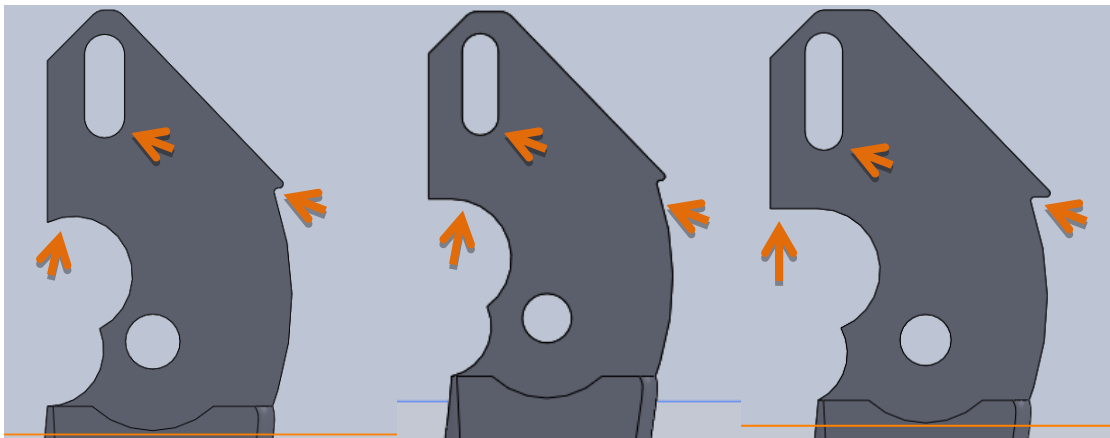


Figure 49. From left to right, stages 1, 2, and 3 of the redesigned Kerrison handles.

The first handle was identical to the handle used for the adjustable model. This is due to the fact that the crossbar has yet to be sharpened, and thus the ratios of the slots to the pins are the same. These handles enable the stage sharpening of our new design. These new handles vary in height and width of the handle as well as the slot to ensure proper mechanics at all the stages.

5.1.1 Assembly

SolidWorks allows you to combine all your parts into one assembly to function as a whole with the use of mates. Concentric mates were used on hinges in order to show the effects of a hinged

part. Mating the crossbar screw tangentially to the slot enables the transfer of motion from the handle to the crossbar. Surface coincidence mates were used to ensure a flush finish along edges while distance limiting mates were used to enforce the keyways. With all the correct mates in place, by moving one part, the actual motion of Kerrison can be simulated. **Error! Reference source not found.** shows an assembly of the cross bar, shank and handle.

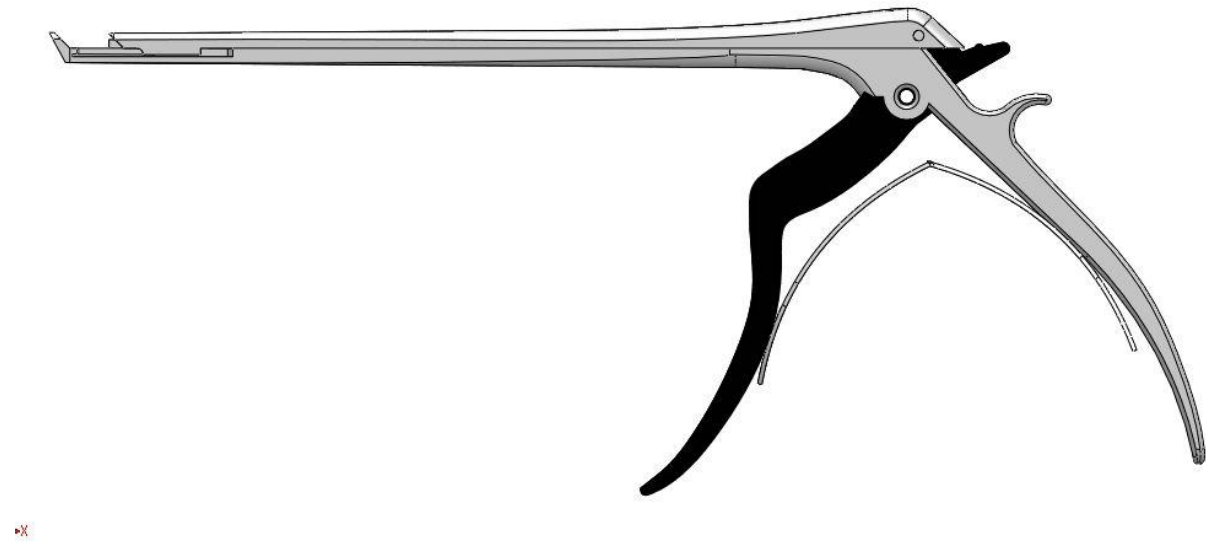


Figure 50. Assembly of crossbar, Shank and Handle.

5.2 Finite Element Analysis of Crossbar

As seen in section 3.2 earlier, we were able to use FEA to confirm the data collected during experimental portions of this project. Using FEA to simulate loads on the 3D CAD generated model, we were able to verify that the strain gage data collected was accurate.

Not only was FEA used to verify experimental results, but it was also vital in identifying the weak points in our design. Beyond that, it allows for testing different solutions under the exact same loading conditions to find the optimal solution. An example of this is shown below in Figure 51, where FEA was used on the crossbar. The figure showed a large stress concentration at the beginning of the first keyway.

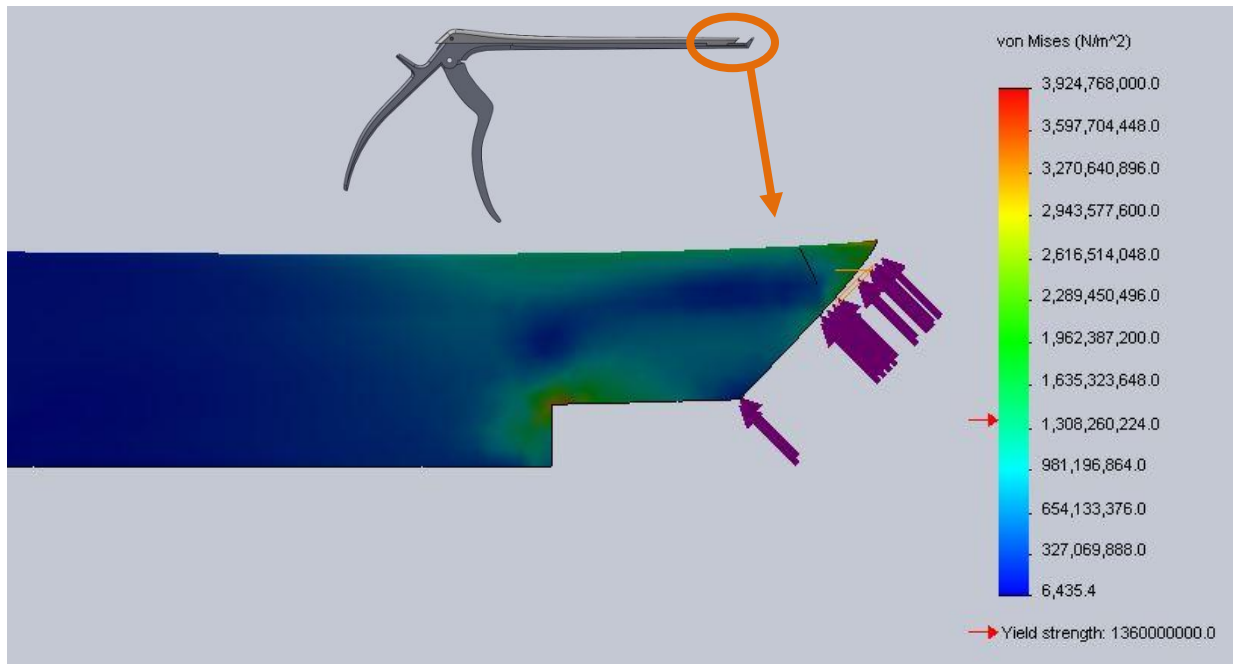


Figure 51. Using FEA to identify stress concentrations in our design.

We decided to incorporate a filleted corner instead of a 90° corner to reduce the amount of stress experienced at that location. We then ran FEA on the proposed solution shown in Figure 52.

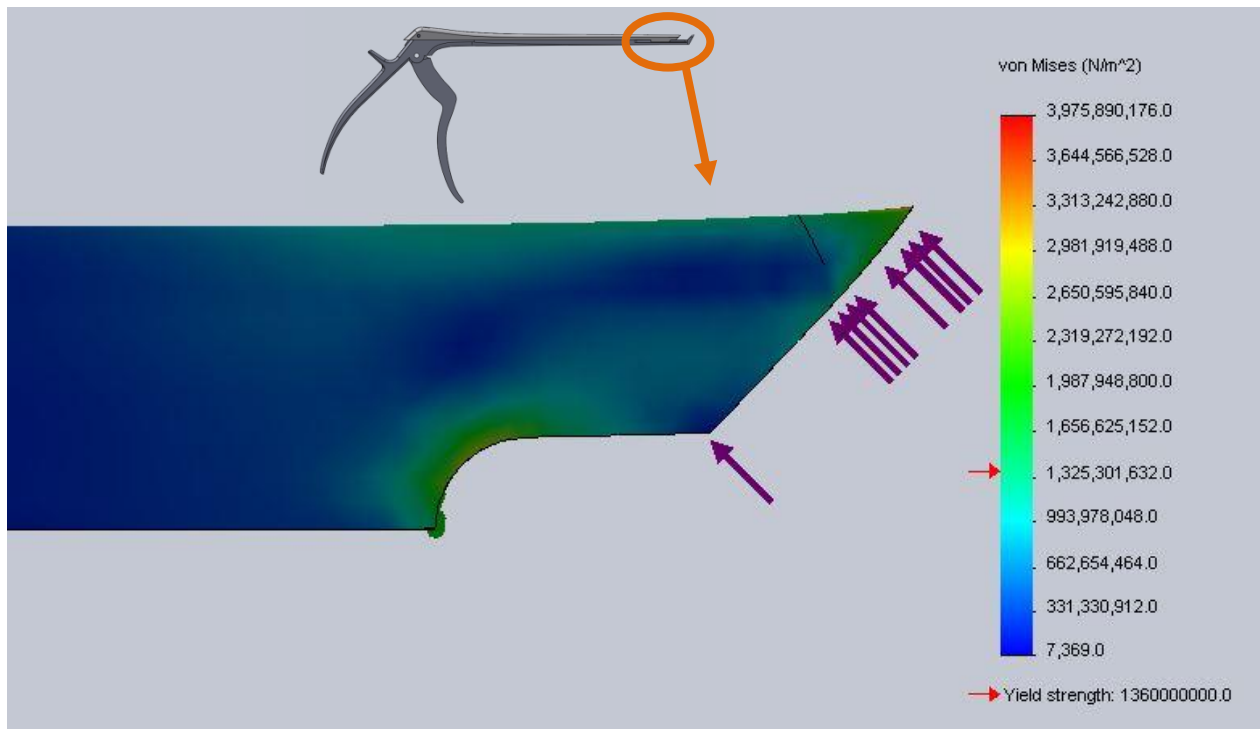


Figure 52: FEA of stresses in cutting tip with filleted key

FEA shows that the stress concentration has been decreased at the corner. Running FEA using 500N (Approximately half the maximum possible applied force) shows that the maximum Von Mises stress is still above the material's yield stress. This is not considered to be a problem because in reality, 1000N would only be considered as a worst case scenario. Human bone has a compressive strength of 170 MPa [9] and shear strength of 51.6 Mpa [10]. Since the yield strength of 420 martensitic stainless steel is 1.36 GPa [6], the Kerrison material is nearly 10 times the strength of human bone. Therefore, it is assumed that the bone will yield and be cut much sooner than the Kerrison would be deformed. The only way the Kerrison would be subjected to loads as high as 1000N is if it is used improperly, where the user squeezes far harder than is necessary to cut the bone or tissue. Another situation when more than expected loads will be applied is when the cutting tip is dull and becomes a blunt blade attempting to cut tissue. If the tissue does not cut the user may apply excessive force resulting in deformation. A solution to keep the blade sharp at all times is explained in section 4.2.2, and will eliminate the possibility of over loading due to dullness.

Lastly, we used FEA to examine the differences in the deformation found at the midpoint of the crossbar between the old and the current Kerrison design. The old Kerrison used a single keyway as compared to the current Kerrison which utilizes a two keyway design. We will identical simulations of each of the two Kerrison designs in order to compare the results. Figure 53 below uses the colors to represent the amount of displacement that will occur during loading. Using the scale on the right of the figure we can relate the colors to a finite amount of displacement. It can be clearly seen that the centre of the crossbar deflects a substantial amount in the single keyway old Kerrison design. The dark red represents 0.2654 mm of displacement.

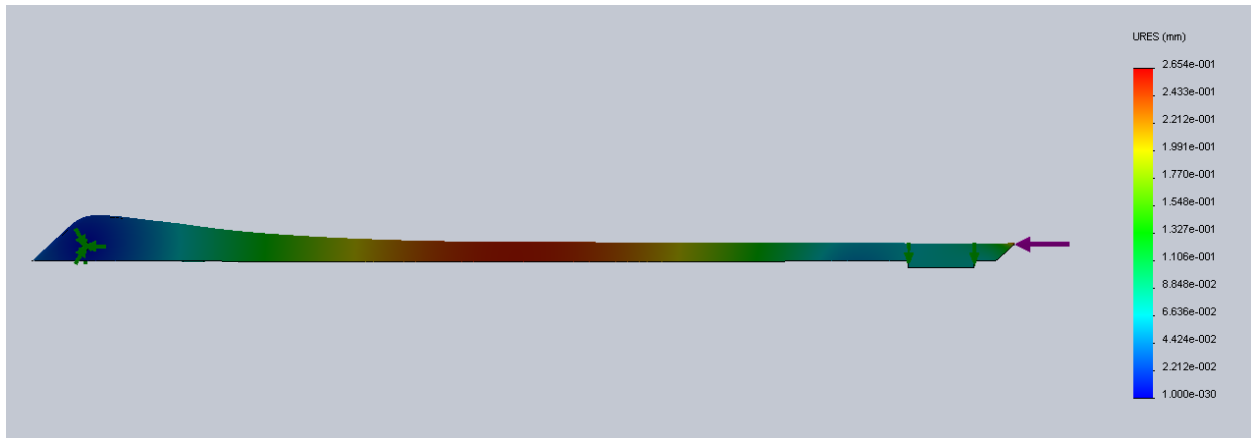


Figure 53. Using FEA to examine the deformation of the mid section of the crossbar of the old Kerrison design.

We then looked at the amount of displacement occurring in the center of the two keyway current Kerrison design shown in Figure 54 below. There is significantly less displacement in the mid crossbar under the exact same loading situation.

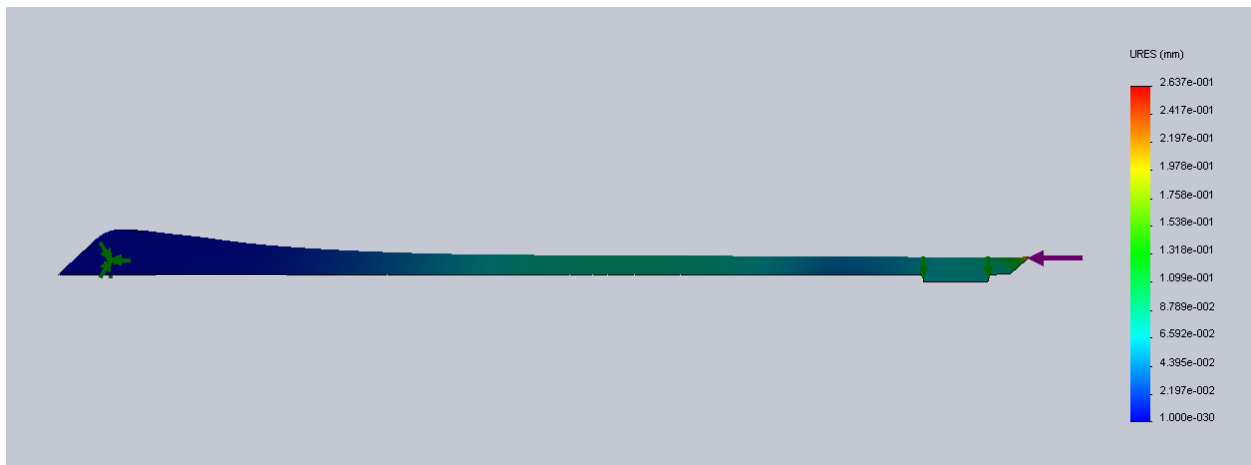


Figure 54. Using FEA to examine the displacement of the mid section of the crossbar of the current Kerrison design.

This FEA simulation was the deciding factor for us to use two keyways instead of just one in our new design. The second keyway clearly reduces the bowing deformation that was occurring over time, and keeping it in the new design makes the most sense moving forward.

5.3 Force Transfer Analysis

During the process of cutting the crossbar inevitably experiences a vertical component of force F_Y when the crossbar pin is not directly above the shank pin.

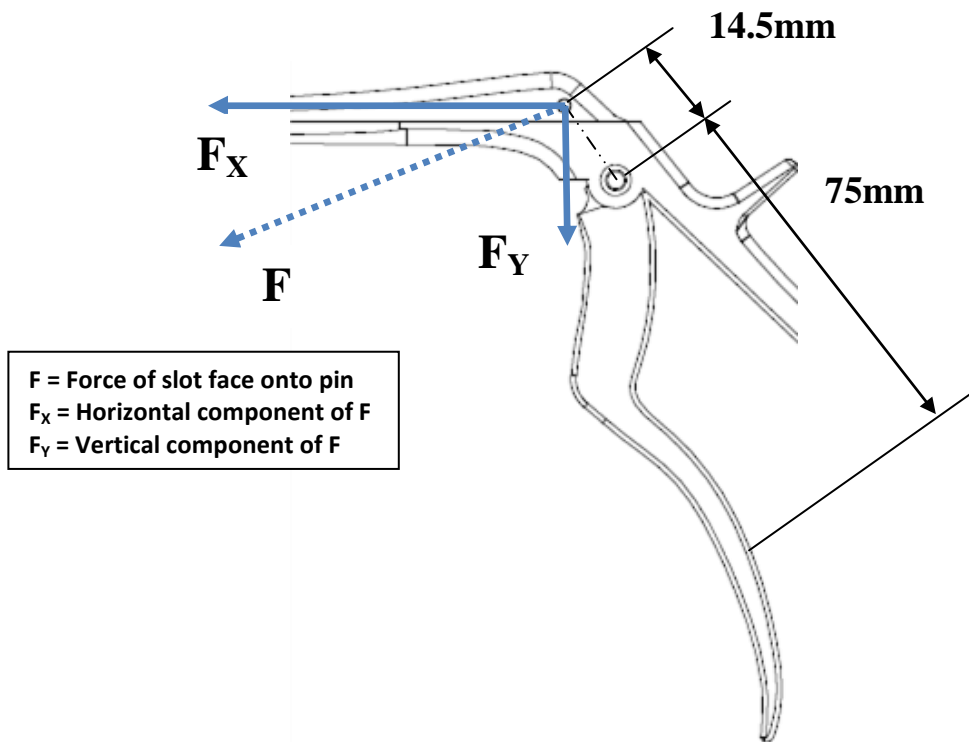


Figure 55. User-applied force components.

Mathematically the component of force that is translated in the horizontal direction, F_x , is given as:

$$F_x = F \cos \theta$$

Here θ is the angle measured between the vertical and the line formed by connecting the crossbar pin to the handle pin. F is the equivalent force transferred to the crossbar resulting from applying a force at the handle, and F_x is the horizontal component of F . The transferred force F can be given as:

$$F = \frac{75\text{mm}}{D} F_A$$

Where F_A is the applied force on the handle and D is the distance from the crossbar pin to the handle pin. The value of 75mm represents the approximate distance from the handle pin to the point of force application on the handle. The point of application was assumed to be the center of the distributed load resulting from a hand squeeze.

The distance from the crossbar pin to the handle pin can be expressed as a function of θ as follows:

$$D = \frac{14.5\text{mm}}{\cos\theta}$$

Where the value of 14.5mm represents the vertical distance from the crossbar pin to the handle pin. Finally, the horizontal component of force transferred through the crossbar as a function of θ is:

$$F_x = \frac{75}{14.5} F_A \cos^2\theta = 5.17 F_A \cos^2\theta$$

The following figures depict three stages of the cutting action, beginning with the rest position (Figure 56), followed by the mid-cut position where the two pins are in a vertical line (Figure 57) and finally the fully compressed position where the blade meets the anvil (Figure 58)

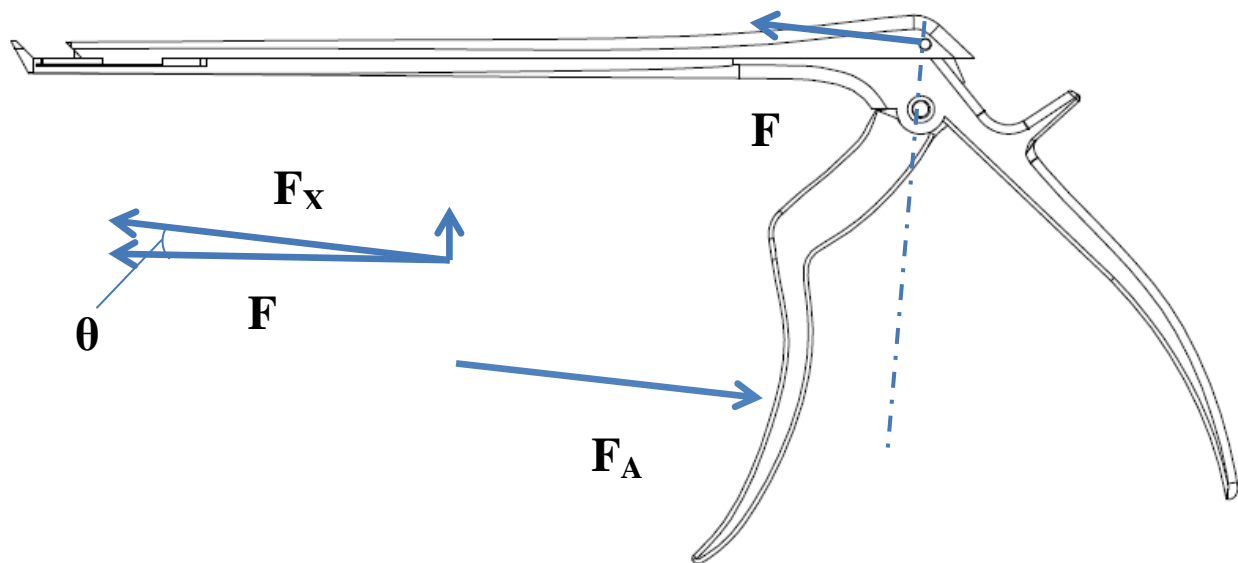


Figure 56. Force transfer angle in rest position.

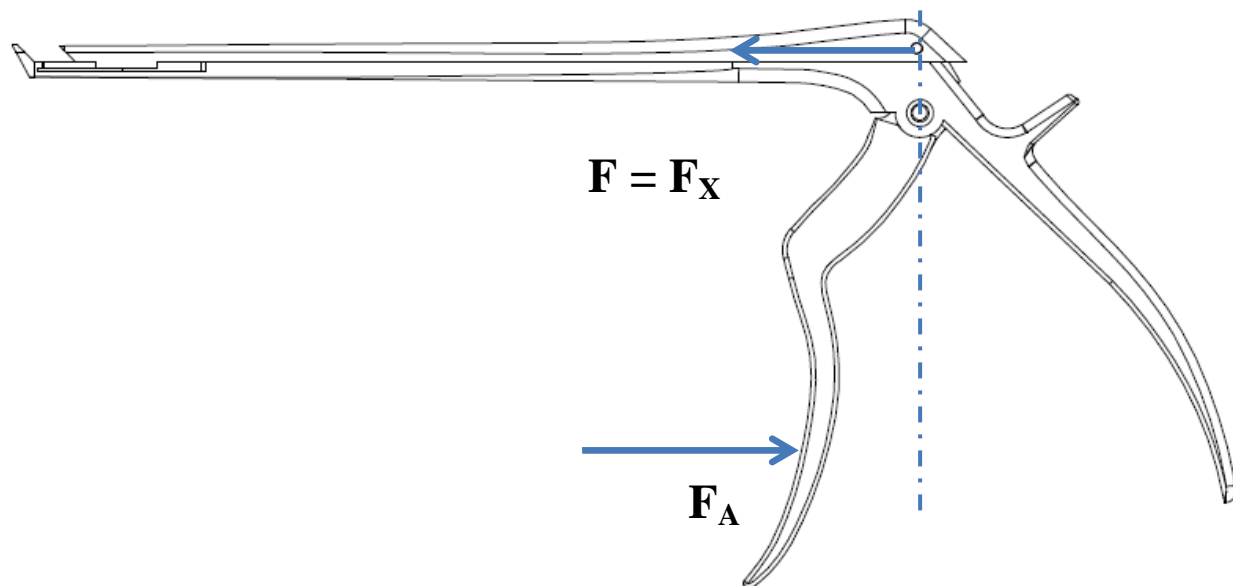


Figure 57. Force transfer angle in mid-cut position.

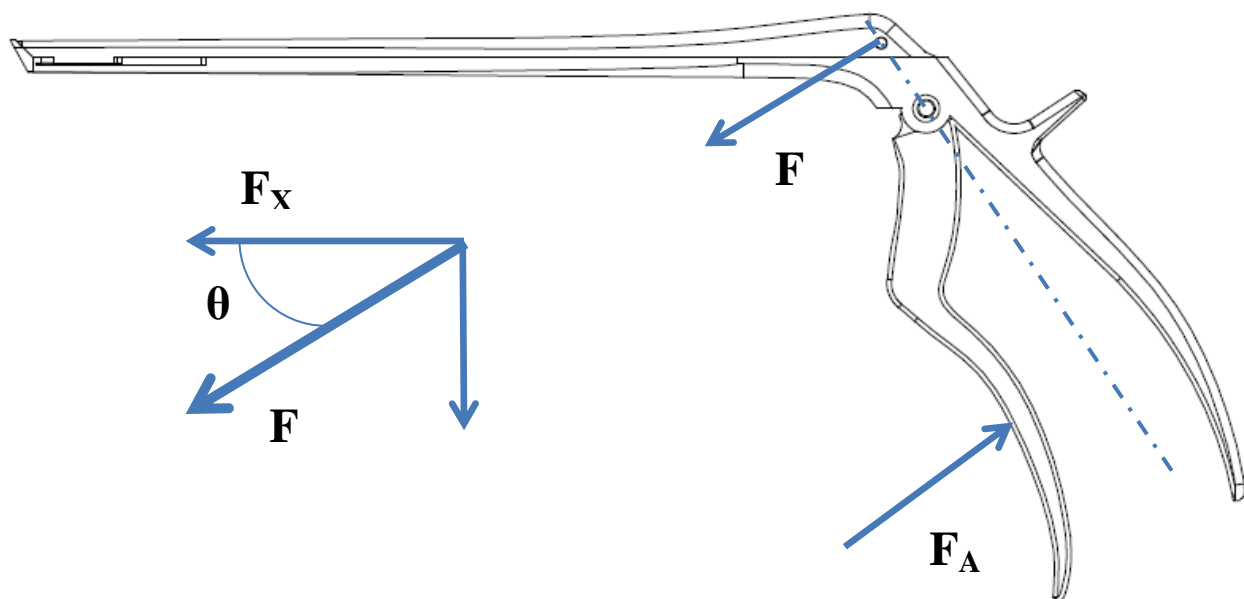


Figure 58. Force transfer angle in fully-compressed position.

From these figures it can be seen that the force applied on the pin is not always parallel to the crossbar. This results in a non-uniform transfer of force along the crossbar during a biting action. When the force is initially applied on the handle by a surgeon's hand, the angle θ is approximately 10° . Using the above equations, the resulting horizontal force component F_x is equal to approximately $5.01F_A$ for an angle of 10° . That is, the transferred force through the

crossbar is approximately five times the applied force by the hand. At the mid-cut position, where θ is 0° , the horizontal force component is approximately $5.17F_A$. Therefore, there is little difference in the force distributed along the crossbar from the rest position to the mid-cut position.

Once the cutting action continues and the pin passes through the mid-cut position, the angle θ begins to increase. This gradually reduces the force transferred horizontally along the crossbar. At the end position where the blade meets the anvil, the angle θ is approximately 30° . This corresponds to a horizontal force component of approximately $3.47F_A$, a significant reduction in cutting force. While this value still indicates an amplified force through the crossbar of nearly four times the applied load, it would still be desirable to maintain a higher coefficient of force amplification.

A possible deterrent to this phenomenon is to increase the length of the crossbar while keeping the shank length constant. This would slightly decrease the maximum value for θ , but would reduce the space in which material could be placed in the tool for cutting. A more logical solution would be to shorten the shank and crossbar in order to decrease the maximum angle θ can reach. This would ultimately decrease the overall length of the tool.

5.4 Finite Element Analysis of Handles

Each handle stage was analysed with Solidworks FEA software to determine the distribution of stresses throughout the thin-walled structure. A force of 1000N was used as the input to match the 1000N magnitude used in previous FEA trials. The 1000N represents the force applied onto the face of the slot by the pin at the top of the handle. The results of the FEA solution for the first stage handle are shown in Figure 59.

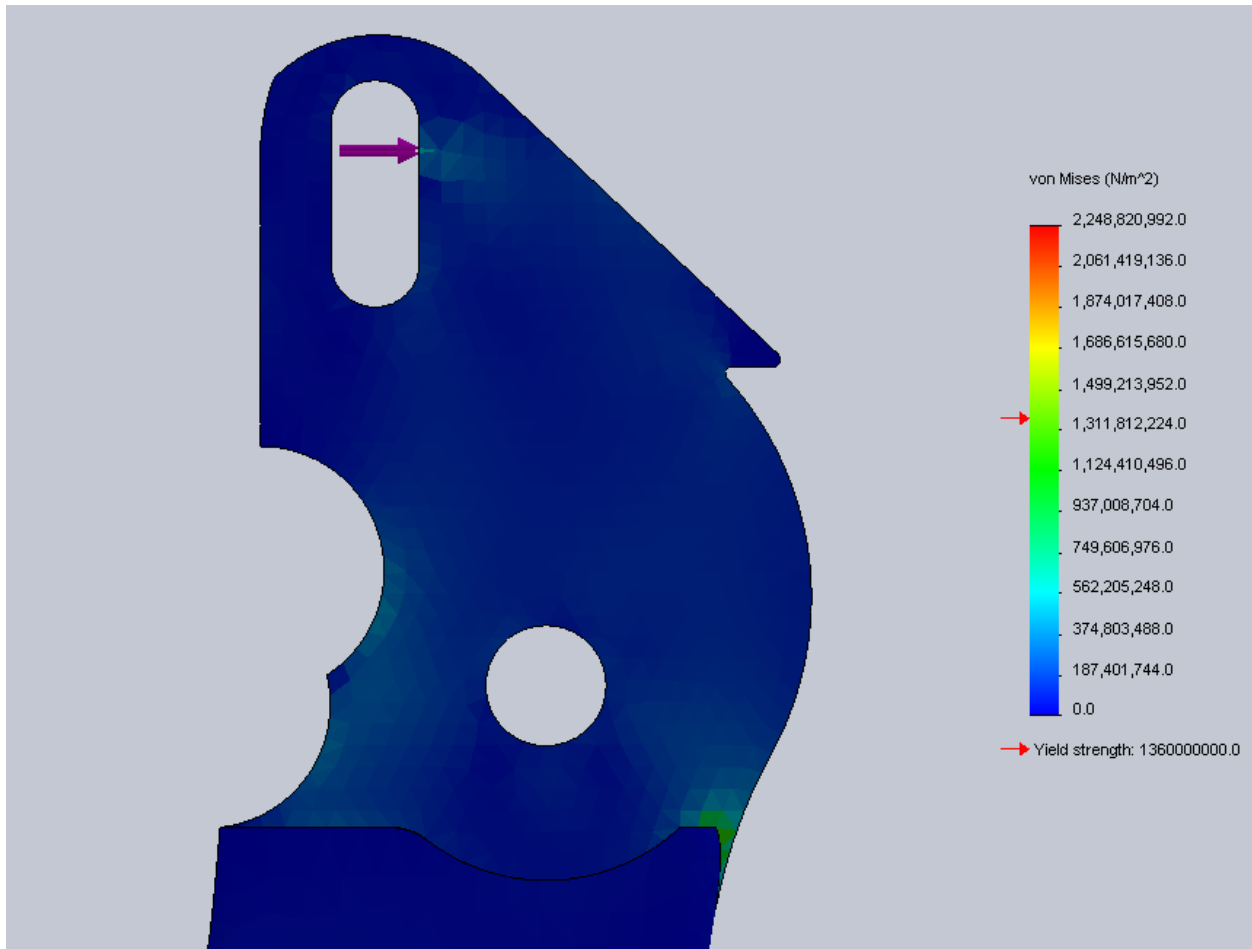


Figure 59. Stress distribution throughout the thin member of the first stage handle.

In Figure 59 the distribution of stresses is noticeably concentrated near the point of force application and along the curved portions at the base of the thin-walled member. Overall, the concentrations of stresses do not appear to exceed the yield strength of the chosen 420 martensitic stainless steel. The design for the first stage handle should be sufficient to withstand any force exerted by the hand during a cutting action. Similar FEA trials were carried out for the second and third handle stages. The results are shown in Figure 60 and Figure 61, respectively.

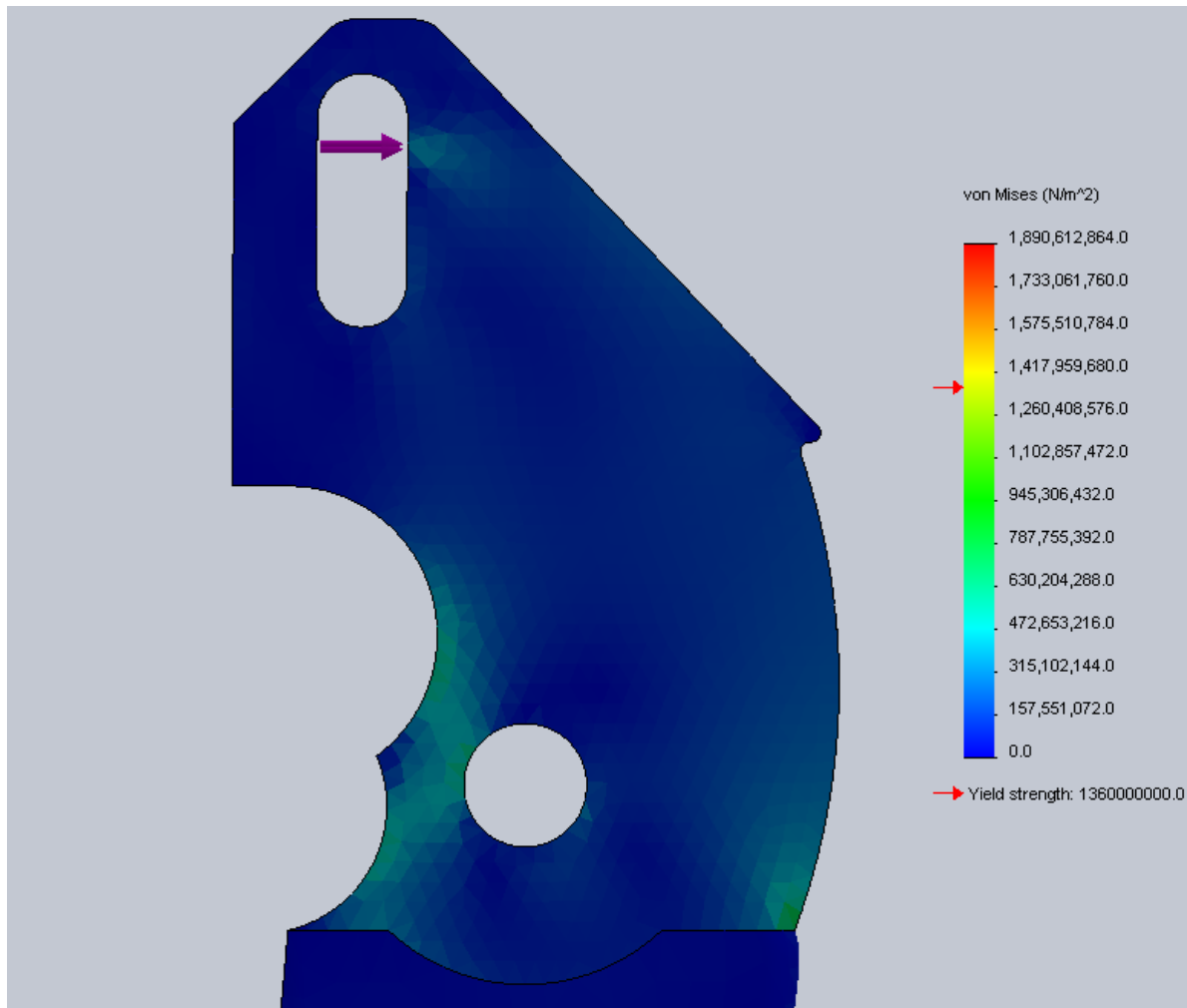


Figure 60. Stress distribution throughout the thin member of the second stage handle.

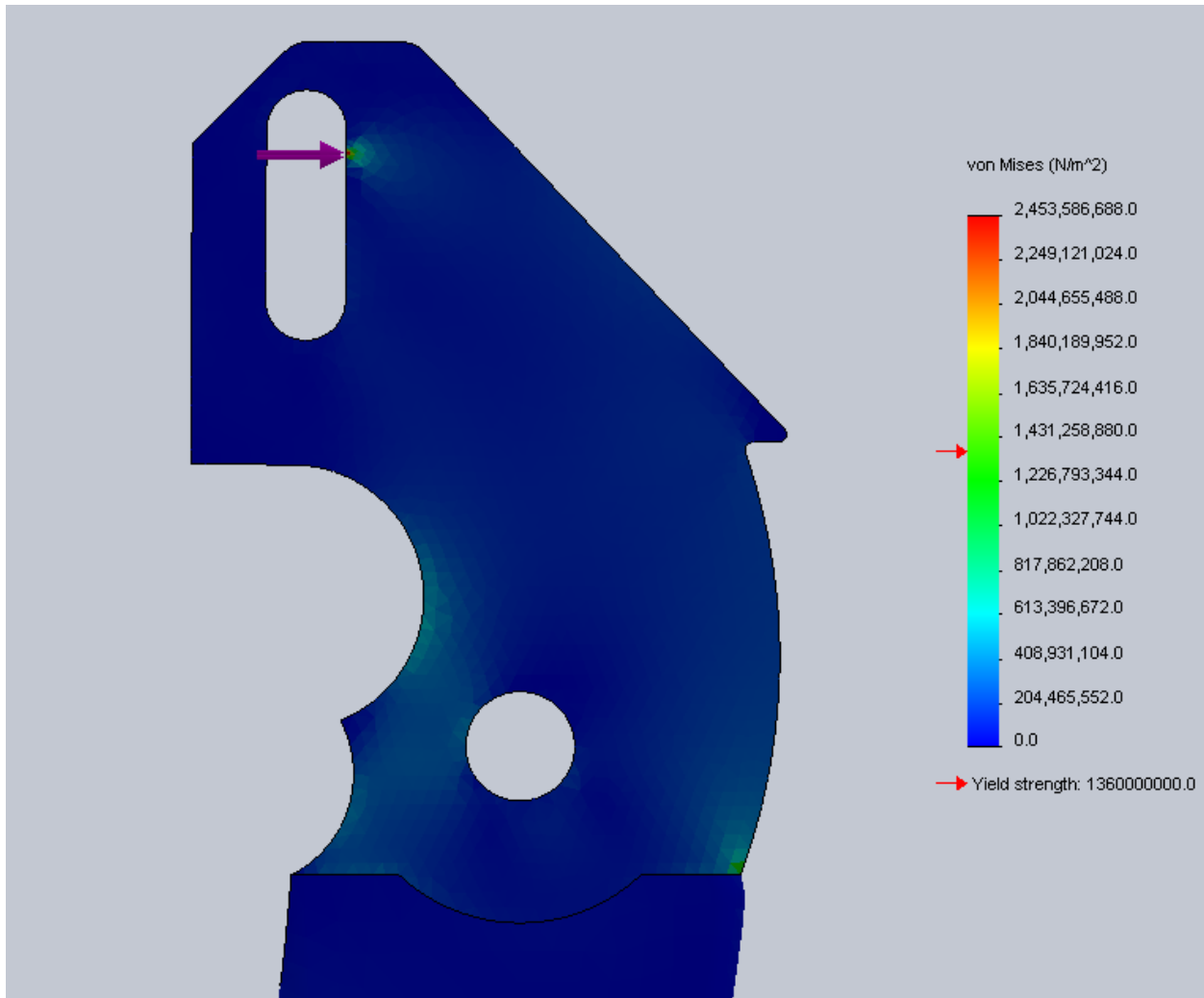


Figure 61. Stress distribution throughout the thin member of the third stage handle.

It can be noticed that the stress concentrations along the circular edges and at the base of the thin-walled member are slightly diminished as we move from the first handle stage to the second and third. This is likely due to the increased amount of material behind the slot to carry the load transferred by the pin. Regardless, the still-present stress concentrations along the curved portions and at the pin contact do not appear to exceed the yield strength of the new material.

5.5 Sterilization Compatibility

A major issue with the non-detachable Kerrisons is the inability to be easily incorporated into the standard sterilization processes. The Kerrison had to be disassembled by technical staff and then inserted into the cycle in pieces, which was a repetitive and time-consuming task. The newer detachable models are easily disassembled with the incorporation of a hammer component. The

inclusion of the hammer feature is an effective solution as it allows for quick and easy disassembly prior to sterilization, as well as easy reassembly.

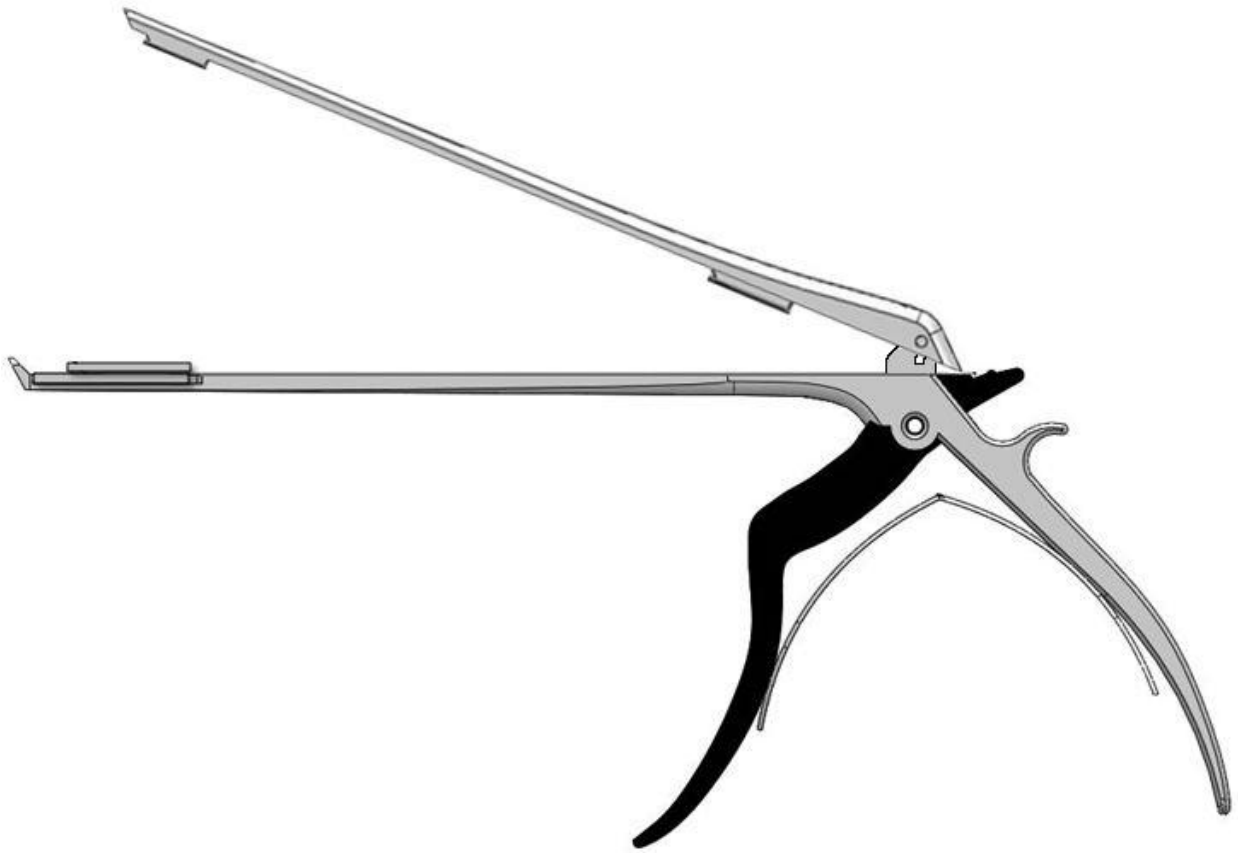


Figure 62. Detachable Kerrison showing opening ability for standardized cleaning and sterilization

Our redesign of the Kerrison incorporates the same hammer feature as described earlier. The mechanism has not been altered significantly, and operates in a similar manner as the current model. Due to this feature as well as the fact that the size and shape of the redesigned Kerrison is maintained from the current models, this new model would be compatible with the previous sterilization methods [1-2].

5.6 Cost Analysis

Depending on the material and complexity of the design, the standard Kerrison Surgical tools cost on average between \$400-\$700. The scope of this project identifies a desired cost of \$500 to \$600 per tool. This project has focused on developing solutions for areas of the current Kerrison's that are failing. By developing these solutions, the client is better able to choose

future Kerrison's which are less susceptible to failure. It is not within the scope of this project to perform a cost analysis on the manufacturing process to build the proposed Kerrison. Since similar Kerrison's do exist, the expected cost of purchasing a similar Kerrison would be in the range of \$500 to \$700.

6 Conclusion

A primary orthopedic spinal surgery tool, the Kerrison bone rongeur, at the Health Sciences Center in Winnipeg MB was experiencing deformation at the cutting tip and was rendered unfit for service in the operating room. Solutions to the problem were required in order to ensure the ability to perform surgeries with the tool in the future.

Tip deformation was verified and the behaviour of the Kerrison was observed through experimental testing using strain gages and a load cell. Five aspects of redesign were created for the Health Sciences Center, three of which are recommended to directly deal with solving the problem of tip deformation. Firstly, a linear drive mechanism comprised of a slotted channel in which a pin interacts and moves the crossbar to make the cut provides a linear application of force and improves the cutting mechanism. Secondly, multiple handles with different linear drive slot locations prolong the life of the tool by enabling more sharpening of the crossbar tip. Thirdly, the material choice for the tool was recommended to be a 420 martensitic stainless steel with Molybdenum for the best hardness, strength and good corrosion resistance, as well as multiple alternating coatings of Titanium Nitride and Zirconium Nitride. Lastly, for better ergonomics when holding and working with the tool, a redesigned curved hand rest was implemented as an additional improvement to the Kerrison. The cutting tip bite height will not be reduced to minimize the forces at the top of the cutting tip that induce deformation as FEA studies showed tip bite height reduction to have little impact on the stresses in the cutting tip.

This redesigned Kerrison will show improvements in its durability, service life, and overall comfort and enjoyment of use.

7 References

- [1] CSA Effective Sterilization in Health Care Facilities by the Steam Process, CSA Standard Z314.3-09, March 2009
- [2] CSA Decontamination of Reusable Medical Devices, CSA Standard Z314.8-08, March 2008
- [3] N. Tu (private communication, photographs used with permission), Sept. 29, 2011.
- [4] *ASM Handbook Volume 3 Alloy Phase Diagrams*. Materials Park, OH: ASM International, 1992.
- [5] Matweb Material Property Data. (2011). *410 Stainless Steel* [Online]. Available: <http://www.matweb.com/search/datasheet.aspx?MatGUID=e5556cce22794269972d2718806a8bc7> [Nov. 24, 2011].
- [6] Matweb Material Property Data. (2011). *420 Stainless Steel* [Online]. Available: <http://www.matweb.com/search/DataSheet.aspx?MatGUID=641544e4c9f1425390d05ae37d55440a> [Nov. 24, 2011].
- [7] Azom.com (2001, Oct. 23). *Stainless Steel – Grade 420* [Online]. Available: <http://www.azom.com/article.aspx?ArticleID=972> [Nov. 24, 2011].
- [8] PF ONLINE (2000, Jul. 1). *PVD Coatings for Medical Device Applications* [Online]. Available: <http://www.pfonline.com/articles/pvd-coatings-for-medical-device-applications> [Nov. 24, 2011].
- [9] K. Schmidt-Nielsen, *Scaling: Why is animal size so important?*. Cambridge, UK: Cambridge University Press, 1984.
- [10] Turner, C.H.; Wang, T.; Burr, D.B.: "*Shear Strength and Fatigue Properties of Human Cortical Bone Determined from Pure Shear Tests*". *Calcified Tissue International* 69 (6): 373–378. doi:10.1007/s00223-001-1006-1. PMID 11800235, 2001.

Appendix A – Concept Selection

The following appendix outlines our project’s concept selection phase for the redesign of the Kerrison as presented prior in our Concept Design Report.

Design concepts were generated through individual brainstorming sessions which resulted in three separate areas for solutions dealing with the cutting tip, the force transfer mechanism and the ergonomics of the tool.

The concept scoring method was chosen to identify which concepts to pursue because of its ability to give weight to the more important selection criteria. The scoring tables for the cutting tip concepts and the ergonomic concepts are given below as TABLE VIII and TABLE IX respectively.

Scoring criteria were determined through consultation with the client and lead users. The weights for each criterion were assigned by perceived importance through discussions with the client. The scoring process was done by committee, with the pros and cons of each concept debated and decided upon by the group.

TABLE VIII CUTTING TIP CONCEPT SCORING

Cutting Tip Concepts			A		B		C		E		F	
Rank	Selection Criteria	Weight	Rate	Weighted	Rate	Weighted	Rate	Weighted	Rate	Weighted	Rate	Weighted
3	Sharpness	18%	4	0.72	4	0.72	4	0.72	5	0.9	5	0.9
1	Durability	25%	2	0.5	1	0.25	5	1.25	3	0.75	2	0.5
2	Ease of Cleaning	20%	2	0.4	3	0.6	5	1	5	1	5	1
5	Sharpenability	11%	5	0.55	1	0.11	4	0.44	2.5	0.275	1	0.11
5	Ease of Manufacturing	11%	3	0.33	1	0.11	2	0.22	1	0.11	3	0.33
4	Ease of Assembly	15%	1	0.15	3	0.45	3	0.45	2	0.3	3	0.45
Total			2.65		2.24		4.08		3.335		3.29	
Rank			4		5		1		2		3	
Continue?			No		No		Yes		Maybe		Maybe	

TABLE IX CUTTING TIP CONCEPT KEY

Letter	Concept
A	Threaded rod concept
B	Screw-driven expanding latch concept
C	Staged sharpened tip concept
D	Anvil blade concept
E	Scalpel-type replaceable blade concept
F	Shearing cutting blade concept

Note that concept D is not included in the scoring. As the scoring and ranking process was underway, concept D was seen to be complementary to any of the other cutting tip concepts that would be implemented and relatively simple to add to any concept. Because of this universal quality of concept D it initially was going to be included with the final design, regardless of what concept was chosen. Thus the scoring and ranking of concept D was not necessary. The reduced bite height concept was also not included in the cutting tip scoring process as it was also going to be incorporated into the final design.

From the scoring process shown in TABLE VIII it was determined that concept C, the staged sharpened tip with multiple handles for crossbar placement, would be pursued for further development as it had the highest weighted score of 4.08 according to the selection criteria and weighted values for each criteria. Concept E, the scalpel-type blade, and concept F, the shearing cutting blade, remained in consideration for future development because of their high weighted scores, however the final design did not include these concepts.

Similar concept scoring and ranking processes took place for the ergonomic concepts shown in TABLE X and TABLE XI. Concepts A and D were chosen for further development towards a final design because of their high scores. Two concepts were chosen instead of just one because of a desire to make the most improvements possible in an effective way. Concepts A and D were not in conflict with each other in terms of what aspects of the existing Kerrison design they would modify and were also relatively simple to implement. The simplicity of both concepts and the improvements they would bring to the final design lead to both of their selections, however concept D, was later dropped and just concept A was developed

TABLE X ERGONOMICS CONCEPT SCORING

Ergonomics Concepts			A		B		C		D	
Rank	Selection Criteria	Weight	Rate	Weighted	Rate	Weighted	Rate	Weighted	Rate	Weighted
2	Comfort	30%	4	1.2	4	1.2	3	0.9	3	0.9
3	Durability	25%	5	1.25	2	0.5	3	0.75	5	1.25
1	Ease of Cleaning	35%	5	1.75	3	1.05	3	1.05	5	1.75
4	Ease of Manufacturing	10%	4	0.4	3	0.3	2	0.2	4	0.4
Total			4.6		3.05		2.9		4.3	
Rank			1		3		4		2	
Continue?			Yes		No		No		Yes	

TABLE XI ERGONOMICS CONCEPT KEY

Letter	Concept
A	Rounded hand stop
B	Padded handles
C	Handle ribs concept
D	Finger groove concept

From the scoring process shown in TABLE X, concepts A and D were chosen for further development towards a final design because of their high scores. Two concepts were chosen instead of just one because of a desire to make the most improvements possible in an effective way. Concepts A and D are not in conflict with each other in terms of what aspects of the existing Kerrison design they would modify and are also relatively simple to implement. The simplicity of both concepts and the improvements they would bring to the final design led to both of their selections.

After the concept generation and scoring, the staged tip sharpening, sharpened anvil, tip height reduction, rounded hand stop and finger groove concepts were chosen. The scalpel-type replacement blades and the shearing cutting blades were also kept in consideration. The only concepts that were incorporated in the final design from this concept generation phase were the staged tip sharpening and the rounded hand stop. The concepts that were added to be included in the final design were a linear transfer mechanism and a material recommendation.

Appendix B – Strain Gage Specifications

Strain gage information provided by manufacturer in strain gage packaging

VISHAY VISHAY MICRO-MEASUREMENTS & SR-4®
General Purpose
STRAIN GAGES

FOR COMPLETE TECHNICAL DATA, VISIT WWW.VISHAY.COM/REF/STRAINAGAGES

GRID RESISTANCE IN OHMS		TC OF GAGE FACTOR, 1%/100°C
350.0±0.3%		(+1.3±0.2)

GRID	GAGE FACTOR @ 24°C	TRANSVERSE SENSITIVITY
1	2.130±0.5%	(+0.2 ±0.2)%
2		
3		
NOM		

ORDER	THERMAL OUTPUT COEFFICIENTS FOR 2024-T4 Aluminum	
	FAHRENHEIT	CELSIUS
0	-1.30E+2	-4.86E+1
1	+3.26E+0	+3.42E+0
2	-2.33E-2	-6.18E-2
3	+4.45E-5	+2.60E-4
4	0.00 E+0	0.00 E+0

FOIL LOT NUMBER A62AF835	BATCH NUMBER CF477467
-----------------------------	--------------------------

ITEM CODE	QUANTITY	CODE
17732	5	203214

MADE IN UNITED STATES



CEA-13-250UW-350/P2

Appendix C – Search Results

The following appendix outlines our project's patent and competitor products search results for the redesign of the Kerrison as presented prior in our Concept Design Report.

Patents

Obtaining information regarding Kerrison patents was accomplished by searching the online patent databases for the Canadian Intellectual Property Office (CIPO) and the United States Patent and Trademark Office (USPTO). Other patent databases, including Faqs.com and Patentgenius.com, yielded similar results but were regarded as secondary sources. As previously stated, most available patents were largely similar, save for varying characteristics in the designs of the crossbar, handles and drive mechanism. While the patent for the current model used by HSC was located, information regarding specific material and geometry characteristics was not provided. In addition, a large number of Kerrison patents exhibited a variety of designs for the cutting tip and drive mechanism, some of which were similar to our own internally-generated concepts. An example of a common feature in our search results was a slot-drive mechanism, though many patents exhibit varying geometrical characteristics. Our own concept for the drive mechanism will be presented further in this report. Certain designs including air-powered cutting mechanisms and integrated suction were dismissed after consultation with the client who determined that such options would be deemed too costly or simply unnecessary for the surgeons.

The client has decided that the various features from our patents searches are not to be considered for implementation. Inclusion of any such features would pose the risk of infringement on the existing patents. For simplicity, our client decided that the final design should remain as geometrically similar as possible to the current

Competitor Products

Our research regarding Kerrison rongeurs offered by competing manufacturers yielded relatively less useful information than our patent search. This is due to the fact that the material and operational specifications are notoriously difficult to obtain from manufacturer websites.

Information regarding geometries, material coatings and instrument strength was largely unattainable. Compared to our patent database searches, the existing competitor products more closely resemble the rongeurs currently in use by HSC. Both the detachable and non-detachable Kerrison rongeurs are currently available through various manufacturers. Prominent manufacturers appearing in our search results included Aesculap, V. Mueller, Boss Instruments Ltd., and JEDMED. Various rongeurs available from V. Mueller and Boss Instruments Ltd. are currently employed by HSC, though newer products from each manufacturer are available. Similarly to our patent search, the more noticeable differences between our search results and the currently used models consisted of aesthetic design and the drive mechanism. The designs of many Kerrison rongeurs were noted to target ease of disassembly and sterilization, and the corresponding concepts for achieving this goal were largely similar to concepts generated in our internal search.

It was noted that many of the concepts discovered through our patent search currently do not seem to exist on the market, or at least have not been manufactured in large enough numbers to maintain a strong presence in manufacturers' profiles.